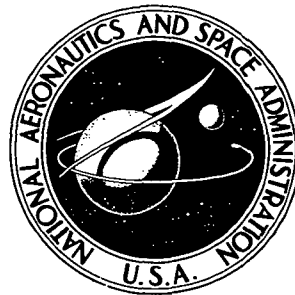


N72-31882

NASA TECHNICAL NOTE



NASA TN D-6948

NASA TN D-6948

**CASE FILE  
COPY**

# GRUMMAN H-33 SPACE SHUTTLE ORBITER AERODYNAMIC AND HANDLING-QUALITIES STUDY

*by Robert W. Rainey, George M. Ware, Richard W. Powell,  
Lawrence W. Brown, and David R. Stone*

*Langley Research Center  
Hampton, Va. 23365*

NATIONAL AERONAUTICS AND SPACE ADMINISTRATION • WASHINGTON, D. C. • SEPTEMBER 1972

1. Report No. NASA TN D-6948		2. Government Accession No.		3. Recipient's Catalog No.	
4. Title and Subtitle GRUMMAN H-33 SPACE SHUTTLE ORBITER AERODYNAMIC AND HANDLING-QUALITIES STUDY				5. Report Date September 1972	
				6. Performing Organization Code	
7. Author(s) Robert W. Rainey, George M. Ware, Richard W. Powell, Lawrence W. Brown, and David R. Stone				8. Performing Organization Report No. L-8379	
9. Performing Organization Name and Address NASA Langley Research Center Hampton, Va. 23365				10. Work Unit No. 502-37-01-06	
				11. Contract or Grant No.	
				13. Type of Report and Period Covered Technical Note	
12. Sponsoring Agency Name and Address National Aeronautics and Space Administration Washington, D.C. 20546				14. Sponsoring Agency Code	
15. Supplementary Notes In addition to the authors of this paper, Thomas A. Blackstock, A. B. Blair, Jr., William A. Corlett, M. Arnold Emmons, Jr., Jerry Humble, and Bernard Spencer, Jr., comprised the Langley Research Center team.					
16. Abstract  A study of a representative delta-wing orbiter, the Grumman H-33, that utilized external-hydrogen tanks has been completed at the Langley Research Center. The study encompassed a detailed wind-tunnel program from subsonic to hypersonic speeds, analyses of the data, and the calculation and assessment of the orbiter handling qualities using the most aft center-of-gravity locations anticipated during entry and approach.					
17. Key Words (Suggested by Author(s)) Space vehicles Aerodynamic characteristics Handling qualities Entry vehicles				18. Distribution Statement Unclassified - Unlimited	
19. Security Classif. (of this report) Unclassified		20. Security Classif. (of this page) Unclassified		21. No. of Pages 46	
				22. Price* \$3.00	

# GRUMMAN H-33 SPACE SHUTTLE ORBITER AERODYNAMIC AND HANDLING-QUALITIES STUDY

By Robert W. Rainey, George M. Ware, Richard W. Powell,  
Lawrence W. Brown, and David R. Stone\*  
Langley Research Center

## SUMMARY

A study of a representative delta-wing orbiter, the Grumman H-33, that utilized external-hydrogen tanks has been completed at the Langley Research Center. The study encompassed a detailed wind-tunnel program from subsonic to hypersonic speeds, analyses of the data, and the calculation and assessment of the orbiter handling qualities using the most aft center-of-gravity locations anticipated during entry and approach. The results showed that longitudinal aerodynamic trim and control were available at attitudes that encompassed the high-cross-range mission. After the angle-of-attack transition maneuver and throughout the regime where aerodynamic pitch, roll, and yaw controls are used (Mach numbers less than about 2), the orbiter was statically longitudinally stable and a simple pitch-rate feedback to the elevons provided acceptable pitch response. Also, generally satisfactory lateral handling qualities were provided with an angular-rate feedback (roll and yaw) and an aileron-to-rudder interconnect.

## INTRODUCTION

During the past several years, NASA and other government and industrial organizations have been developing an efficient and cost-effective transportation system capable of transferring large payloads to and from near-earth orbits. In many of the concepts studied, an orbiter was vertically launched by a winged booster which staged, performed a turnaround entry maneuver, and flew back to the launch site. After staging, the orbiter was flown to orbit and, after completion of the orbital mission, was deorbited. It entered the sensible atmosphere at high angles of attack in essentially a spacecraft mode and during the latter phase of the entry performed an angle-of-attack maneuver to the lower attitude aircraft mode for final acquisition of the landing site and approach and landing. The more recent orbiters studied were clipped-delta-wing-body configurations with relatively

---

\* In addition to the authors of this paper, Thomas A. Blackstock, A. B. Blair, Jr., William A. Corlett, M. Arnold Emmons, Jr., Jerry Humble, and Bernard Spencer, Jr., comprised the Langley Research Center team.

low-fineness-ratio fuselages, large base areas, and far-aft center-of-gravity locations in comparison with conventional aircraft.

As part of a continuing effort to identify the most suitable concept, a study of an orbiter utilizing an external-hydrogen-tank concept has been conducted by the Langley Research Center. With this concept, the low-density hydrogen of the ascent propellant was carried in external tanks and thereby reduced orbiter size and development costs. The orbiter configuration selected for the study was the Grumman Aerospace Corporation H-33 design. The objectives of the study were (1) to provide an experimental base for a representative external-hydrogen-tank concept and (2) to evaluate the orbiter aerodynamic characteristics and handling qualities from hypersonic to subsonic speeds. To meet these objectives, wind-tunnel data were obtained in seven facilities, six at the Langley Research Center and one at the Marshall Space Flight Center. Force tests were conducted from low-subsonic speeds to Mach numbers of about 20 throughout angles of attack that encompassed the predicted operational attitudes for a high-cross-range mission. These data were used with calculated damping derivatives in a preliminary evaluation of handling qualities which are presented in terms of longitudinal and lateral-directional stability and control of the basic airframe and of the basic vehicle with a relatively simple stability augmentation system (SAS).

## SYMBOLS

Measurements and calculations were made in the U.S. Customary Units. They are presented herein in the International System of Units (SI) with the equivalent values in the U.S. Customary Units given parenthetically.

b	reference wing span, meters (ft)
$C_L$	lift coefficient, $\frac{\text{Lift}}{qS}$
$C_l$	rolling-moment coefficient, $\frac{\text{Rolling moment}}{qSb}$
$C_{l_p}$	roll-damping derivative, $\frac{\partial C_l}{\partial (pb/2V)}$
$C_{l_\beta}$	effective dihedral parameter, $\frac{\Delta C_l}{\Delta \beta}$ , per deg
$C_{l_{\delta_a}}$	rolling-moment coefficient due to aileron deflection, $\frac{\Delta C_l}{\Delta \delta_a}$ , per deg
$C_{l_{\delta_r}}$	rolling-moment coefficient due to rudder deflection, $\frac{\Delta C_l}{\Delta \delta_r}$ , per deg
$C_m$	pitching-moment coefficient, $\frac{\text{Pitching moment}}{qS'}$

$C_{mC_N}$	longitudinal static margin, $\frac{\partial C_m}{\partial C_N}$
$C_{m_\alpha} = \frac{\partial C_m}{\partial \alpha}$	
$C_N$	normal-force coefficient, $\frac{\text{Normal force}}{qS}$
$C_n$	yawing-moment coefficient, $\frac{\text{Yawing moment}}{qSb}$
$C_{n_p}$	yawing-moment coefficient due to rolling velocity, $\frac{\partial C_n}{\partial (pb/2V)}$
$C_{n_\beta}$	directional-stability parameter, $\frac{\Delta C_n}{\Delta \beta}$ , per deg
$C_{n_\beta \text{ dyn}}$	dynamic directional-stability parameter, $C_{n_\beta} \cos \alpha - C_{l_\beta} \frac{I_Z}{I_X} \sin \alpha$
$C_{n_{\delta_a}}$	yawing-moment coefficient due to aileron deflection, $\frac{\Delta C_n}{\Delta \delta_a}$ , per deg
$C_{n_{\delta_r}}$	yawing-moment coefficient due to rudder deflection, $\frac{\Delta C_n}{\Delta \delta_r}$ , per deg
$g$	acceleration due to gravity, meters/sec <sup>2</sup> (ft/sec <sup>2</sup> )
$I_Z/I_X$	ratio of moments of inertia about yaw and roll axes, respectively
$K$	ratio of amount of bank angle obtained to amount required in 2 seconds
$L/D$	lift-drag ratio
$l'$	fuselage length, meters (ft)
$M$	free-stream Mach number
$n$	normal acceleration, g units
$p$	rolling velocity, rad/sec
$q$	free-stream dynamic pressure, newtons/meter <sup>2</sup> (lb/ft <sup>2</sup> )
$R_l$	Reynolds number based on fuselage length
$S$	wing area, including portion within fuselage, meters <sup>2</sup> (ft <sup>2</sup> )
$t_{\phi=30^\circ}$	time to bank 30°, sec
$V$	free-stream velocity, meters/sec (ft/sec)
$\alpha$	angle of attack, deg or rad

$\beta$	angle of sideslip, deg
$\delta_a$	aileron deflection, $\frac{\delta_{e,L} - \delta_{e,R}}{2}$ , positive for right roll command, per deg
$\delta_{ap}$	pilot input to aileron deflection, deg
$\delta_e$	elevon deflection, $\frac{\delta_{e,L} + \delta_{e,R}}{2}$ , positive for trailing edge down, deg
$\delta_r$	rudder deflection, $\frac{\delta_{r,L} + \delta_{r,R}}{2}$ , positive for trailing edge left viewed from the rear, deg
$\delta_{rf}$	rudder flare angle, $\frac{\delta_{r,L} - \delta_{r,R}}{2}$ , deg
$\zeta_d$	Dutch roll damping ratio
$\zeta_{sp}$	longitudinal short-period damping ratio
$\tau_R$	roll-mode time constant, sec
$\psi_\beta$	phase angle of the Dutch roll oscillation in sideslip, deg
$\omega_d$	Dutch roll frequency, rad/sec
$\omega_{nsp}$	longitudinal short-period frequency, rad/sec
$\omega_\phi$	undamped natural frequency of numerator quadratic in roll to aileron-input transfer function, rad/sec

Subscripts:

L	left
max	maximum
R	right

Facility abbreviations:

LaRC CFHT – Langley continuous-flow hypersonic tunnel

LaRC 22" He T – Langley 22-inch helium tunnel

LaRC LTPT – Langley low-turbulence pressure tunnel

LaRC 8' TPT – Langley 8-foot transonic pressure tunnel

LaRC UPWT – Langley Unitary Plan wind tunnel

LaRC 20" HT – Langley 20-inch Mach 6 tunnel

MSFC 14" WT – Marshall Space Flight Center 14- by 14-inch trisonic wind tunnel

### CONFIGURATIONS AND FLIGHT REGIMES

The orbiter configuration (ref. 1) is shown in figure 1 and consists of a fuselage approximately 41.2 meters (135 ft) in length (full scale) in combination with a  $55^\circ$  swept delta wing and a vertical tail. The proposed flight control during entry assumed an attitude control propulsion system (ACPS) of sufficient size to provide pitch, roll, and yaw control during high-altitude hypersonic flight where the dynamic pressures were low. During lower altitude hypersonic flight where the dynamic pressures were of sufficient magnitude, mixed-mode control may be required (i.e., both aerodynamic and ACPS). In the supersonic and transonic flight regimes, the conventional aerodynamic controls plus a flared rudder were used. The flared rudder was designed to provide positive  $C_{n\beta}$  increments with a slight increase in longitudinal static stability. The conventional aerodynamic controls were also used at subsonic speeds with the rudders closed to provide boattailing, which reduced base drag.

Predicted orbiter flight attitudes at various Mach numbers (from ref. 1) are shown in figure 2; constant- $\alpha$  entry at  $27^\circ$  provided the  $L/D$  for the high-cross-range mission. The  $\alpha$ -transition maneuver was initiated at Mach 4 with completion near Mach 2, followed by low- $\alpha$  flight ( $\approx 6^\circ$ ) until the final flare was initiated. Entry was performed at a higher  $C_L$  than that for maximum  $L/D$ ; the lower-speed portion of the flight ( $M < 3$ ) was performed at a lower  $C_L$  than that for maximum  $L/D$  (except in final flare), thereby leaving a maneuver capability for limited flight-path corrections.

### MODELS, EQUIPMENT, AND DATA REDUCTION

The models and wind-tunnel facilities used in the investigation are given in table I; facility details are contained in references 2 and 3. Three different size models were tested: 0.0148-scale, 0.00585-scale, and 0.00337-scale. The largest (0.0148-scale)

model which was tested from Mach numbers of 0.25 to 4.63 was complete with the three rocket nozzles in the base. Inner portions of the nozzles were removed, however, for sting clearance. The smaller models were built without nozzles. In all tests, the models were sting mounted, and the aerodynamic forces and moments were measured by internally mounted six-component strain-gage balances. Appropriate wind-tunnel corrections for the various facilities were applied to the data. The data from Mach numbers of 0.25 to 10.2 were reduced with no base-pressure corrections. Data for  $M = 20.3$  had the base pressure corrected to free-stream values because of a positive base pressure caused by the subsonic boundary layer of the sting.

The coefficients were based on model wing area, span, and body length, and the moment data were reduced relative to 66.3 percent of the body length. The facility, the Reynolds number based on body length, the model scale, and the Mach number, in addition to the configuration variables, are included on each of the basic data plots of longitudinal characteristics.

## RESULTS AND DISCUSSION

### Static Aerodynamic Characteristics

Longitudinal. - The wind-tunnel data are presented in figure 3 and show the variation of the aerodynamic coefficients with angle of attack throughout the Mach number range for each elevon deflection angle investigated. Plots of the longitudinal trim characteristics ( $C_m = 0$ ) of the configuration at each Mach number are presented in figure 4.

The data of figure 3(a) show that at low-subsonic speeds ( $M = 0.25$ ), the configuration has a maximum lift-drag ratio of about 7.3 and is longitudinally stable. As transonic speeds are approached ( $M = 0.8$ ), the model exhibited pitch-up tendencies at angles of attack above about  $12^\circ$  with accompanying reductions in stability and control effectiveness. At Mach numbers above about 1.60, the pitching moments are more linear. At  $M = 2.99$ , the pitch-up characteristics have disappeared, and the stability has become neutral throughout the angle-of-attack range.

At hypersonic speeds, data from three facilities were obtained (fig. 3(g)) and exhibit similar trends with a maximum  $L/D$  of approximately 2 and positive stability and control at trim over the angles of attack from maximum  $L/D$  to the highest test values. At a Mach number of 20.3, two models were tested; the larger model (having a scale of 0.00585) was tested up to an angle of attack of about  $30^\circ$ . The results from these tests are in good agreement with the results for the 0.00337-scale model.

At trim (fig. 4), the low-speed maximum  $L/D$  is approximately the same as the untrimmed value (7.3). As the Mach number increases into the low-supersonic regime, the maximum  $L/D$  drops to approximately 2. At transonic speeds, the vehicle is longi-



itudinally stable in the operational angle-of-attack regime but exhibits neutral stability at the higher angles. This neutral stability extends over the entire test angle-of-attack range at Mach numbers of 2.99 and 3.48. At higher speeds, instability is observed at lower angles of attack which are below those envisioned for normal operation. (See fig. 2.) At hypersonic speeds (fig. 4(d)) and at the  $27^\circ$  operational angle of attack, the vehicle is longitudinally stable with an  $L/D$  value of approximately 1.5. The maximum trimmed  $L/D$  was about 2; and the trimmed data for the 0.00585- and the 0.00337-scale models are in excellent agreement.

Lateral-directional stability.- The body-axis lateral-directional stability characteristics are presented in figure 5. At Mach numbers up through  $3\frac{1}{2}$ , the configuration is directionally stable at the operational angles of attack (fig. 2). The abrupt loss in  $C_{l_\beta}$  and the variation in  $C_{n_\beta}$  at subsonic speeds ( $M = 0.25$ ) for  $\alpha > 18^\circ$  are believed to be the result of the scrubbing action of vortices shed at the wing-body juncture which has been noted in other shuttle delta-wing configurations (for example, ref. 4). The consistent reduction in directional stability and effective dihedral as Mach number increases from 1.6 to 10.2 is evident; however, even at hypersonic speeds the vehicle exhibits positive effective dihedral (negative values of  $C_{l_\beta}$ ) and has a positive value of  $C_{n_{\beta_{dyn}}}$  at the envisioned operational angle of attack of  $27^\circ$ . Values of hypersonic lateral-directional stability characteristics at longitudinal trim are presented in figure 6 and exhibit trends similar to those for the untrimmed conditions.

Lateral and directional control.- In the flight regimes where aerodynamic control was specified (previously noted), data were obtained for nominal values of rudder and aileron deflection angles. The data in figures 7 and 8 show that aerodynamic lateral and directional control are available from midsupersonic through subsonic speeds at the operational angles of attack. In the midsupersonic regime where the angle-of-attack transition from  $\alpha = 27^\circ$  to  $6^\circ$  was envisioned (Mach numbers 4 to 2), the yawing moment due to roll control is proverse (fig. 7) as is also true at lower speeds, except at Mach numbers of 0.95 and 1.2. This will be discussed in more detail in the section entitled "Handling Qualities." Although the use of ACPS was anticipated at hypersonic speeds, aerodynamic roll-control data were obtained at a Mach number of 5.96 and 10.2 (fig. 7(e)). As observed on other configurations, the roll-control effectiveness and the yaw due to roll control are functions of the average elevon deflection angle  $\delta_e$ . For hypersonic trim at the operational angle of attack of  $27^\circ$ , an elevon deflection angle of about  $-5^\circ$  is required (fig. 3(g)), and the yaw-roll ratio resulting from roll-control deflection (fig. 7(e)) is about -0.25, indicating potential adverse yaw.

The rudder provides directional control (fig. 8(a)) over the speed range from subsonic to supersonic. Directional-control effectiveness is approximately constant with angle-of-attack variation at lower speeds; the use of  $30^\circ$  of rudder flare at Mach numbers of 1.60 and greater prevents the deterioration in directional control that would have been

associated with an unflared rudder. The directional-control effectiveness at Mach 1.60 with rudder flare is only about 10 percent less than that obtained at Mach 1.20 without rudder flare. At a Mach number of 10.2 (fig. 8(c)), rudder effectiveness was measured and, as anticipated, was lost above an angle of attack of approximately  $20^\circ$  and was very low at maximum  $L/D$  ( $\alpha \approx 15^\circ$ ). As anticipated, some form of ACPS will be required.

Summary comments.- The static aerodynamic characteristics of the configuration are summarized over the speed range by presenting variations of  $L/D$ ,  $C_{mC_N}$ , and  $C_{n\beta_{dyn}}$  with Mach number in figure 9. The results are shown for the vehicle at angles of attack corresponding to the flight profile of figure 2. The unflagged symbols denote trimmed data whereas the flags denote untrimmed data. Also, the Mach number 0.25 data were used at a Mach number of 0.36. In general, the maximum  $L/D$  over the speed range (dashed line) is in excess of the values at the operational angles of attack (symbols) and thereby indicates a small excess performance. Results of an extrapolation of low-subsonic lift-drag ratios from model to full-scale values by altering the skin friction from model to full-scale Reynolds numbers (ref. 5) indicate that the maximum  $L/D$  should increase from 7.3 to about 7.7. The configuration is longitudinally stable (statically) with the exception of a region near Mach number 3 where  $C_{m\alpha} = 0$ . The derivative  $C_{n\beta_{dyn}}$  is positive over the entire Mach number range, and, although data in the lower speed regime are for untrimmed conditions, differences in  $C_{n\beta_{dyn}}$  due to trimming are not expected to be large.

### Handling Qualities

Calculations have been made utilizing three-degree-of-freedom longitudinal and lateral-directional linearized equations of motion to assess the handling qualities of the configuration. The evaluation was made primarily for the aircraft mode of the flight envelope in which the vehicle would be in the atmosphere at low angles of attack where aerodynamic controls are effective and at Mach numbers less than about 3. As previously mentioned, during high-altitude hypersonic flight, ACPS will be used for control. During lower altitude hypersonic flight, a blending of ACPS and aerodynamic controls may be required. The handling characteristics presented in figures 10 to 14 for Mach numbers of 6 and greater are for the vehicle with aerodynamic controls only and, therefore, do not represent the flight control system of the configuration. However, these values are included to represent the basic, unaugmented vehicle handling qualities. The static aerodynamic derivatives used in the evaluation were those presented in the previous sections, and the mass and inertia properties were provided by the Grumman Aerospace Corporation.

In assessing the handling qualities, the requirements assumed are those presented in reference 6 for large, low-to-medium maneuverability airplanes in a cruise, climb, or

descent condition (class III, category B flight phase) since no requirements have been established for space shuttle orbiter configurations. The handling qualities of the unaugmented airframe are labeled "Basic" in figures 10 to 14.

The evaluation of the longitudinal handling qualities was limited to assessing the frequency (fig. 10(a)) and damping (fig. 10(b)) of the short-period mode. In figure 10(a), boundaries are shown for satisfactory, acceptable, and unacceptable frequency characteristics. At frequencies in the upper unacceptable region, there is a tendency for pilot-induced oscillations (PIO); and at frequencies in the lower unacceptable region, the vehicle is sluggish. In general, the frequencies exhibited by the basic airframe were acceptable in the range of  $M \leq 2.16$  and unacceptably sluggish at  $M = 3.0$  (where  $C_{m\alpha} = 0$ ) and at  $M = 6$  and  $10$ . A simple pitch-rate augmentation system provided satisfactory frequencies for the range of Mach numbers below 3 and an acceptable frequency at  $M = 3$ . As shown in figure 10(b), the short-period damping ratio of the basic configuration without a stability augmentation system (SAS) was satisfactory at  $M = 3$  and at subsonic speeds ( $M < 0.8$ ); however, with a pitch-rate damper, the damping was high at  $M = 3$  but satisfactory for low-supersonic and subsonic speeds ( $M < 3$ ).

The lateral-directional handling qualities are presented primarily at  $M \leq 2.16$ . The Dutch roll damping and frequency for the unaugmented configuration was satisfactory at  $M = 1.2$  and below (fig. 11). With a roll-rate and yaw-rate feedback control system, the vehicle had satisfactory Dutch roll modes for Mach numbers  $\leq 2.16$ .

The unaugmented configuration had unsatisfactory roll-mode damping (fig. 12) except at  $M = 0.36$  where it was satisfactory for low  $\alpha$ . There was an increase in the roll-mode time constant with an increase in  $\alpha$  because of the decrease in  $-C_{lp}$  and  $C_{np}$  with  $\alpha$ . (See ref. 1.) A combination of a roll-rate and yaw-rate feedback augmentation system for the supersonic and transonic regimes and a roll-rate feedback augmentation system for the subsonic region gave satisfactory roll damping except at  $M = 1.2$ ; at this Mach number, the adverse-yaw derivative ( $-C_{n\delta_a}$ ) will make it difficult to obtain satisfactory roll damping with a rate feedback control system for this configuration.

The roll-coupling parameter ( $\omega_\phi/\omega_d$ ) is presented in figure 13. Optimum handling occurs when the three-degree-of-freedom response to aileron inputs is a pure roll with no Dutch roll excitation. When  $\omega_\phi/\omega_d = 1$ , there is a minimum of sideslip disturbance. When there are yawing moments due to aileron inputs ( $\omega_\phi/\omega_d$  greater or less than unity), the resulting side accelerations with roll may cause pilot discomfort and insecurity (ref. 7). Reference 7 indicates a small preference for adverse yaw due to aileron inputs ( $\omega_\phi/\omega_d < 1$ ) over favorable yaw due to aileron inputs ( $\omega_\phi/\omega_d > 1$ ). The configuration of the present investigation had, in general, satisfactory values of  $\omega_\phi/\omega_d$  for the design flight attitudes except at  $M = 1.2$  where the aileron yawing moment was adverse ( $-C_{n\delta_a}$ ).

Augmenting the basic configuration with an aileron-to-rudder interconnect ( $C_{n\delta_a}$  augmentor) provided satisfactory values of  $\omega_\phi/\omega_d$  throughout the aerodynamic flight regime ( $M \leq 2.16$ ).

The amount of aileron deflection used for roll control for the unaugmented vehicle was  $10^\circ$ , and the rolling performance was well within the class III, category B requirements throughout the Mach number range (fig. 14(a)). At  $M = 2.16$ , the roll response was slower due to the reduction in the static rolling moment with aileron deflections ( $-C_{l\delta_a}$ ). With augmentation, a portion of the aileron deflection was allocated to roll augmentation, and the time to roll increased slightly. The sideslip excursion during the rolling maneuvers (fig. 14(b)) was well within the requirement for this class of vehicle. The aileron-to-rudder interconnect reduced the sideslip excursions to less than  $2^\circ$  and changed the phase-angle relationship of the Dutch roll oscillation in sideslip,  $\psi_\beta$ . The amount of rudder required with aileron deflections for turn coordination (fig. 14(c)) was relatively small at the mission angles of attack except at  $M = 1.2$  where more rudder was required because of the adverse-yaw condition. As  $\alpha$  increased, the amount of rudder required increased throughout the Mach number range and, in some cases, exceeded 80 percent of the amount of aileron deflection.

## CONCLUSIONS

Static aerodynamic data were obtained from Mach 20 to subsonic speeds on a delta-wing-type shuttle orbiter. From these data, handling qualities were calculated at flight attitudes during entry for the high-cross-range mission and during landing approach. Emphasis was placed upon the speed regime at Mach numbers less than 3, where after the transition maneuver from high to low angles of attack, aerodynamic controls are used for trim, control, and augmentation. From this study, the following conclusions were reached:

1. At each Mach number, static longitudinal trim and control were available at angles of attack that encompassed at least those for the design mission and for maximum lift-drag ratio.
2. Trimmed maximum lift-drag ratios of about 2 at high speeds and 7.3 at low speeds were available. In general, the maximum lift-drag ratios available over the speed range were greater than values at operational angles of attack.
3. At the flight attitudes (angle of attack less than about  $6^\circ$  and Mach numbers less than about 2) after the angle-of-attack transition maneuver, the orbiter was statically longitudinally stable and a simple pitch-rate feedback to the elevons provided acceptable pitch response.

4. At low-subsonic speeds, the effective dihedral parameter dropped abruptly to near zero at maximum lift where the angle of attack was in excess of touchdown attitude.

5. Generally satisfactory lateral handling qualities were provided at low-supersonic to subsonic flight conditions with an angular-rate feedback (roll and yaw) and an aileron-to-rudder interconnect.

6. Roll control was available with proverse yaw except at transonic speeds where adverse yaw was indicated. Yaw control was adequate below transonic speeds.

Langley Research Center,  
National Aeronautics and Space Administration,  
Hampton, Va., August 14, 1972.

#### REFERENCES

1. Anon.: Alternate Space Shuttle Concepts Study. Pt. II – Technical Summary. Vol. II – Orbiter Definition. MSC-03810, B-1 (Contract NAS 9-11160), Grumman/Boeing, July 6, 1971. (Available as NASA CR-115654.)
2. Pirrello, C. J.; Hardin, R. D.; Heckart, M. V.; and Brown, K. R.: An Inventory of Aeronautical Ground Research Facilities. Vol. I – Wind Tunnels. NASA CR-1874, 1971.
3. Simon, Erwin: The George C. Marshall Space Flight Center's 14 × 14 Inch Trisonic Wind Tunnel Technical Handbook. NASA TM X-53185, 1964.
4. Freeman, Delma C., Jr.; and Ellison, James C.: Aerodynamic Studies of Delta-Wing Shuttle Orbiters. Pt. I – Low Speed. Vol. III of Space Shuttle Aerothermodynamics Technology Conference, NASA TM X-2508, 1972, pp. 785-801.
5. Jacobs, Eastman N.; and Sherman, Albert: Airfoil Section Characteristics as Affected by Variations of the Reynolds Number. NACA Rep. 586, 1937.
6. Anon.: Flying Qualities of Piloted Airplanes. Mil. Specif. MIL-F-8785B(ASG), Aug. 7, 1969.
7. Harper, Robert P., Jr.: In-Flight Simulation of the Lateral-Directional Handling Qualities of Entry Vehicles. WADD Tech. Rep. 61-147, U.S. Air Force, Nov. 1961.

TABLE I. - MODELS AND WIND TUNNELS UTILIZED

Facility	Reference	Scale	Mach no. range	Reynolds no. range, per m	Angle-of-attack range, deg
LaRC LTPT	2	0.0148	0.25	$7.87 \times 10^6$ to $43.96 \times 10^6$	-1 to 24
LaRC 8' TPT	2	0.0148	0.6 to 1.2	$13.12 \times 10^6$	-1 to 24
LaRC UPWT	2	0.0148	1.6 to 2.16	$6.56 \times 10^6$	-2 to 30
LaRC UPWT	2	0.0148	2.30 to 4.63	$8.20 \times 10^6$	-4 to 32
MSFC 14" WT	3	0.00337	1.4 to 5.0	$17.32 \times 10^6$ to $27.43 \times 10^6$	0 to 20
LaRC 20" HT	2	0.00585	6.0	$12.96 \times 10^6$	10 to 45
LaRC CFHT	2	0.00585	10.2	$3.31 \times 10^6$	0 to 45
LaRC 22" He T	2	0.00585	20.3	$14.47 \times 10^6$	14 to 30
LaRC 22" He T	2	0.00337	20.3	$14.47 \times 10^6$	16 to 48

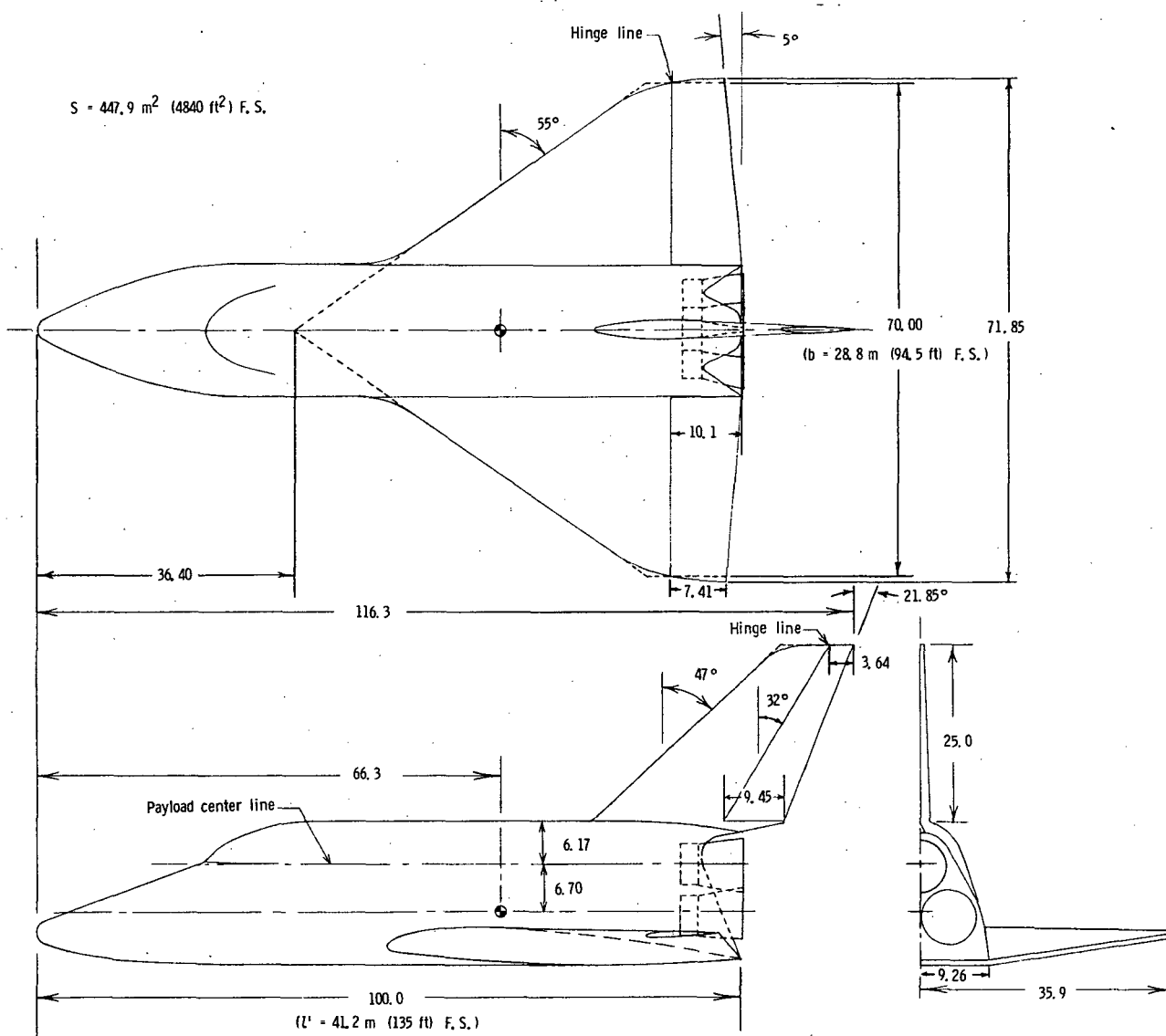


Figure 1. - Grumman H-33 orbiter.

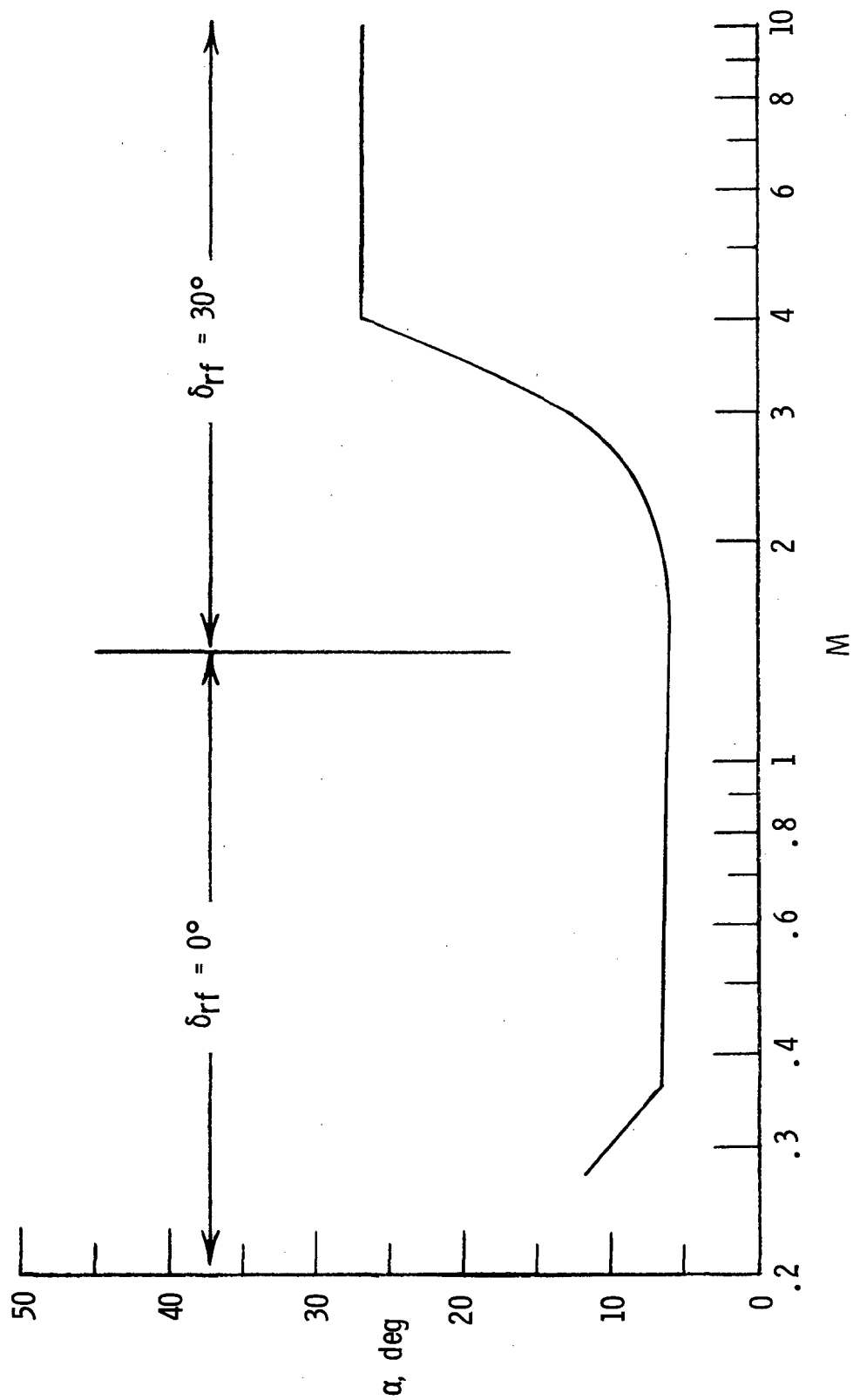
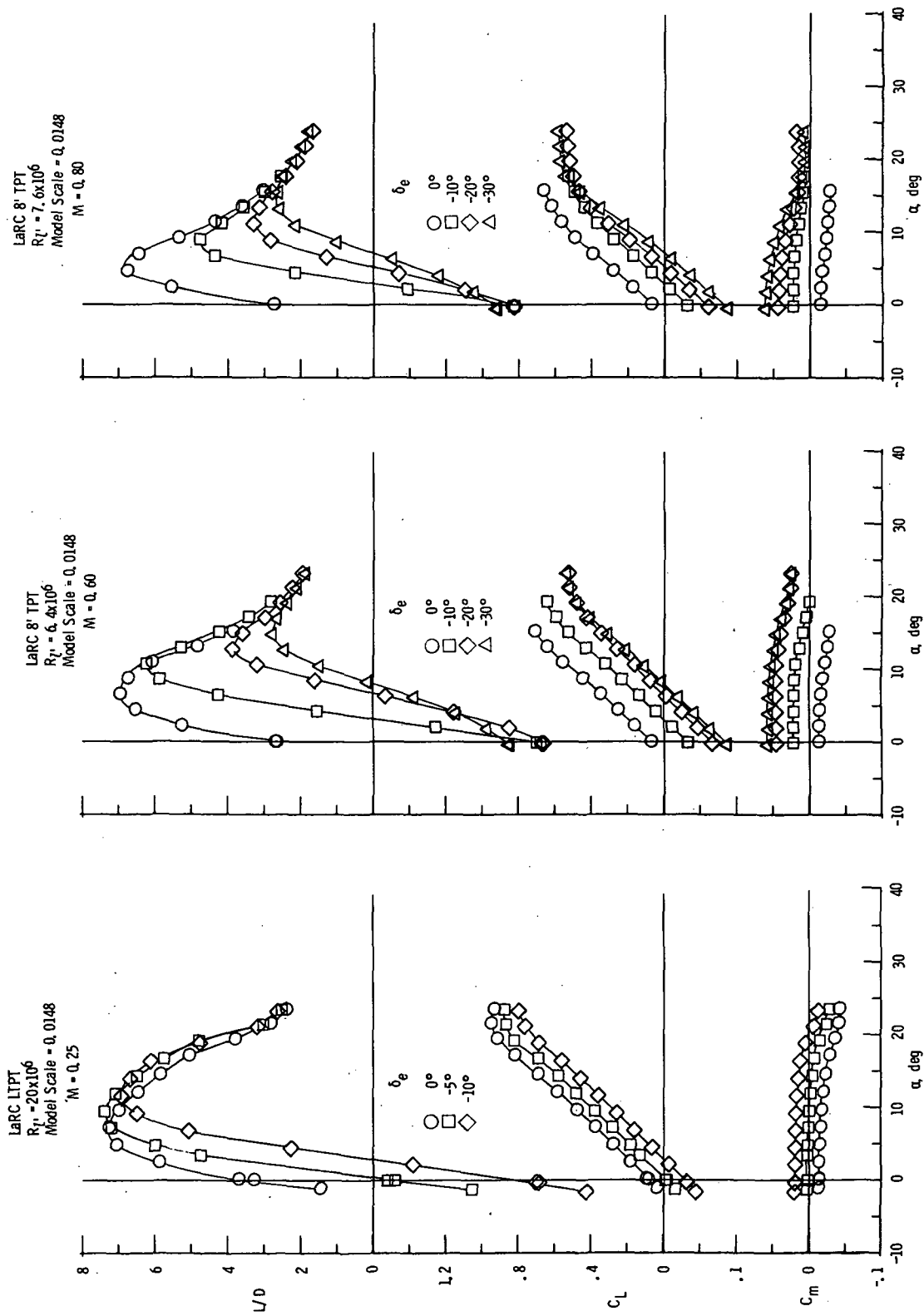


Figure 2.- Nominal operational  $\alpha$ -schedule for high-cross-range mission (ref. 1).

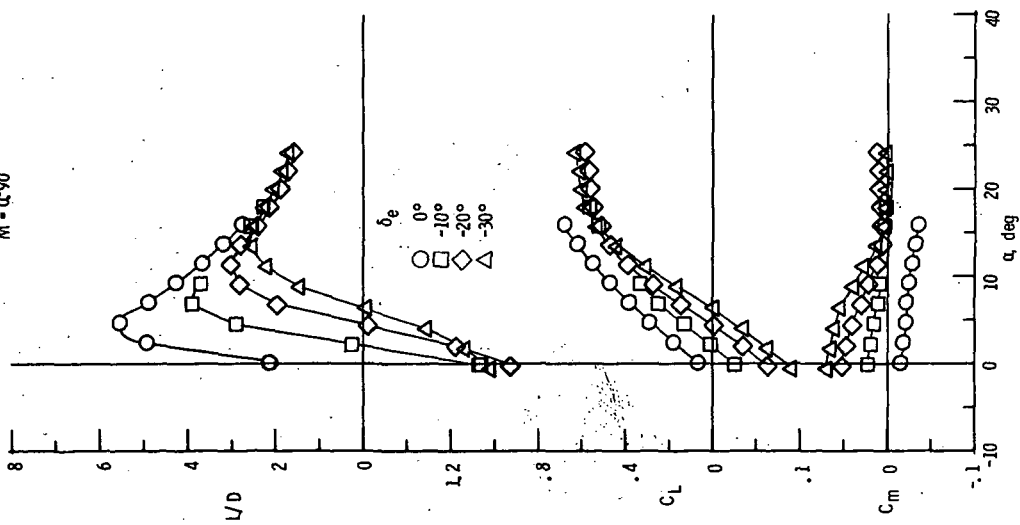




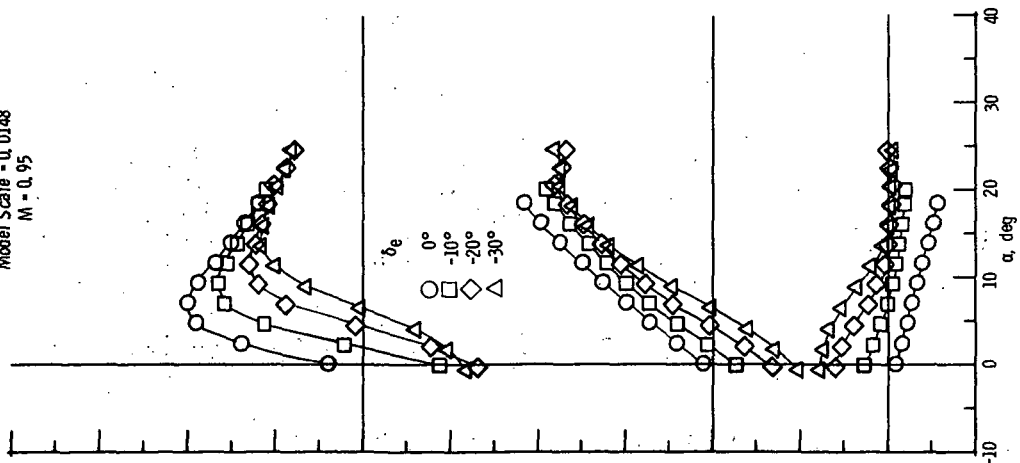
(a)  $0.25 \leq M \leq 0.80$ ;  $\delta_{rf} = 0^\circ$ .

Figure 3.- Longitudinal aerodynamic characteristics.  $\delta_r = 0^\circ$ .

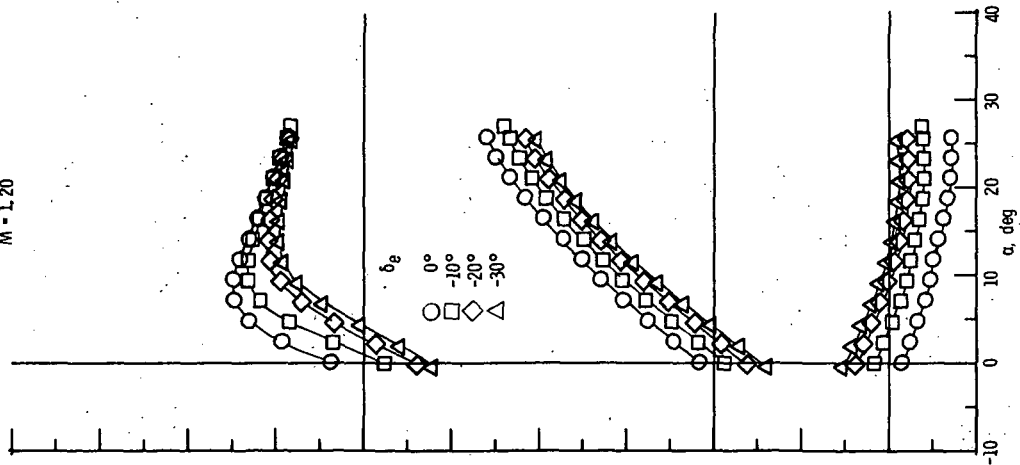
LaRC 8' TPT  
 $R_T = 8.0 \times 10^6$   
 Model Scale = 0.0148  
 $M = 0.90$



LaRC 8' TPT  
 $R_T = 8.1 \times 10^6$   
 Model Scale = 0.0148  
 $M = 0.95$



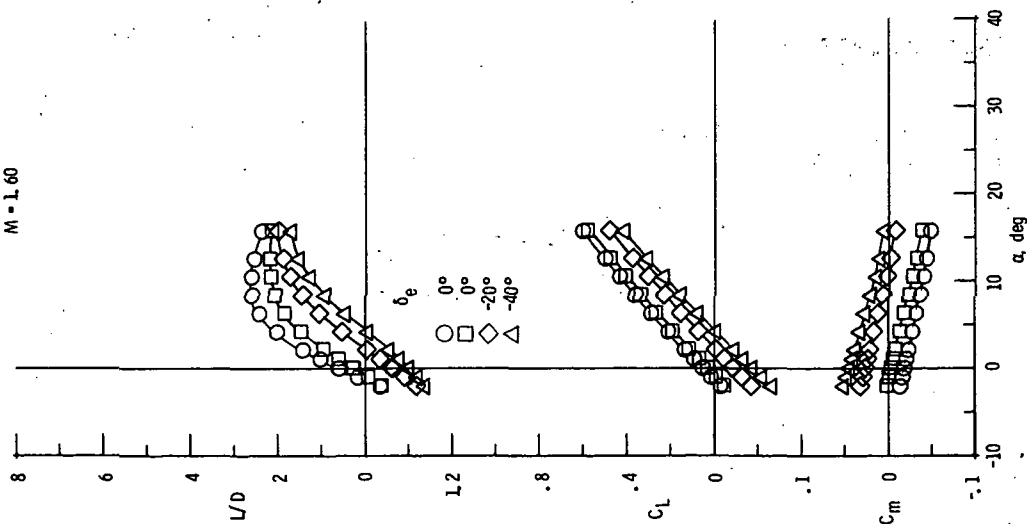
LaRC 8' TPT  
 $R_T = 8.5 \times 10^6$   
 Model Scale = 0.0148  
 $M = 1.20$



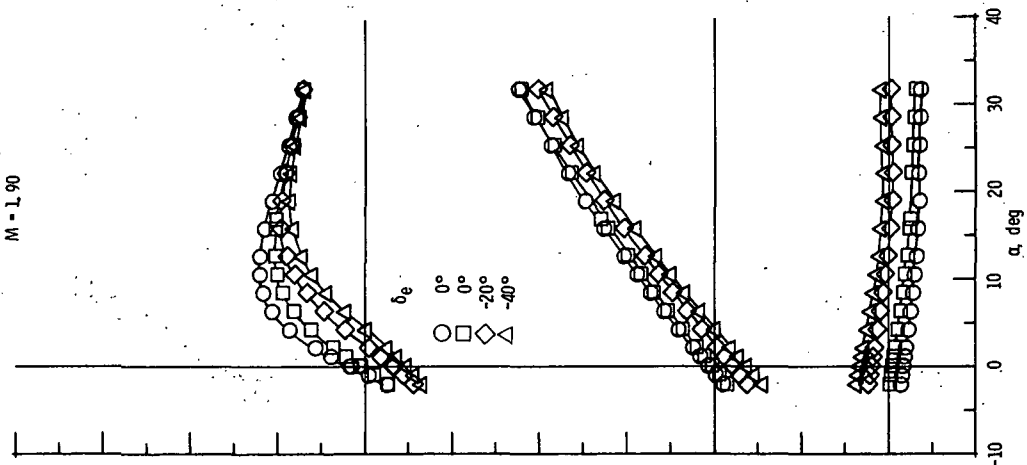
(b)  $0.90 \leq M \leq 1.20$ ;  $\delta_{rf} = 0^\circ$ .

Figure 3.- Continued.

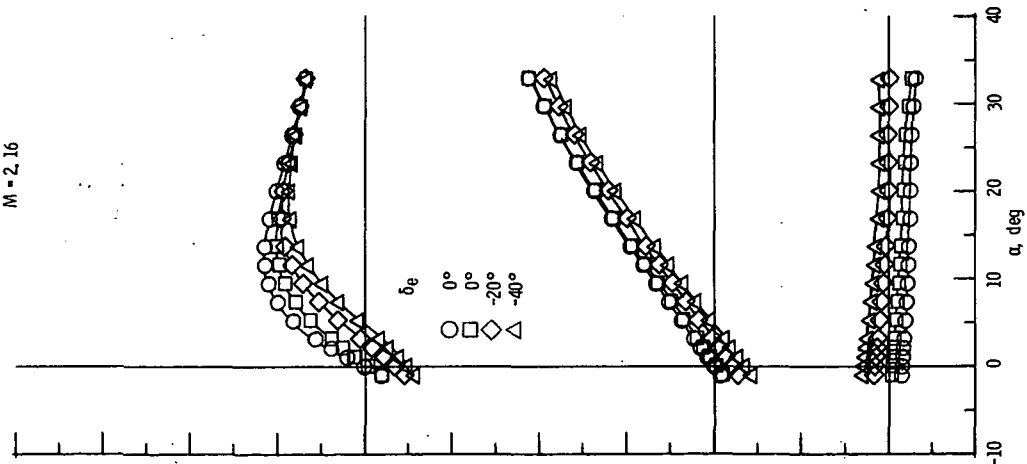
LaRC UPWT  
 $R_{f1} = 3.5 \times 10^6$   
 Model Scale = 0.0148  
 $M = 1.60$



LaRC UPWT  
 $R_{f1} = 3.5 \times 10^6$   
 Model Scale = 0.0148  
 $M = 1.90$

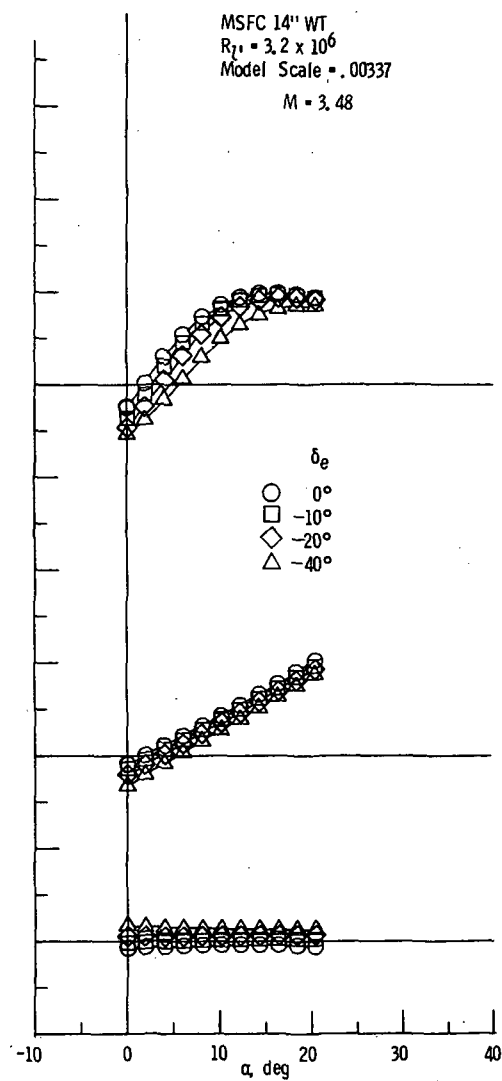
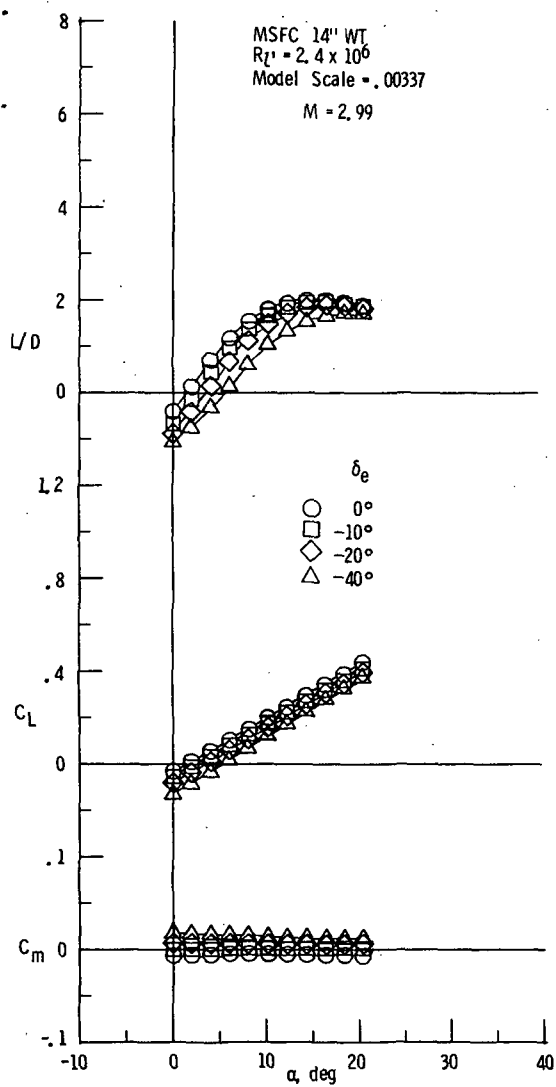


LaRC UPWT  
 $R_{f1} = 3.5 \times 10^6$   
 Model Scale = 0.0148  
 $M = 2.16$



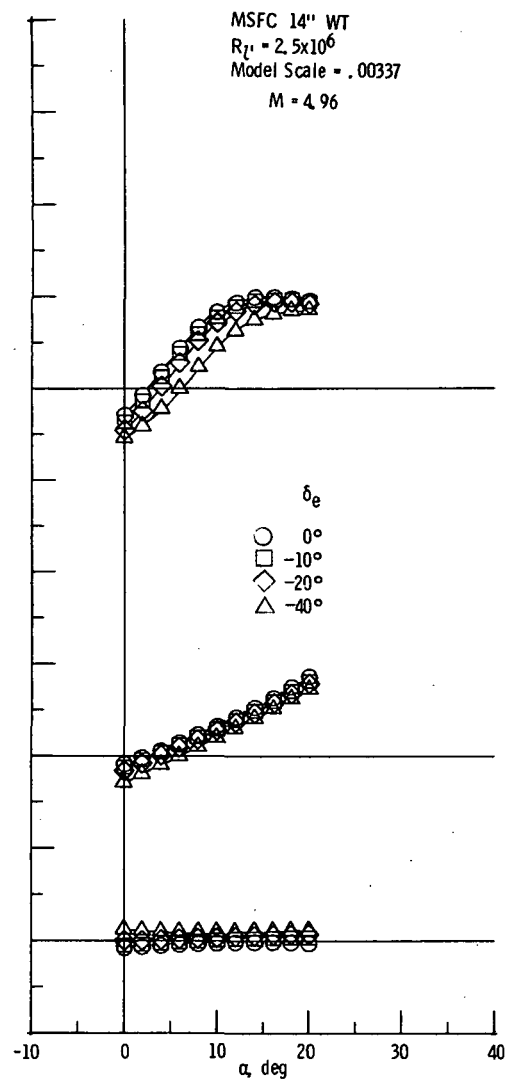
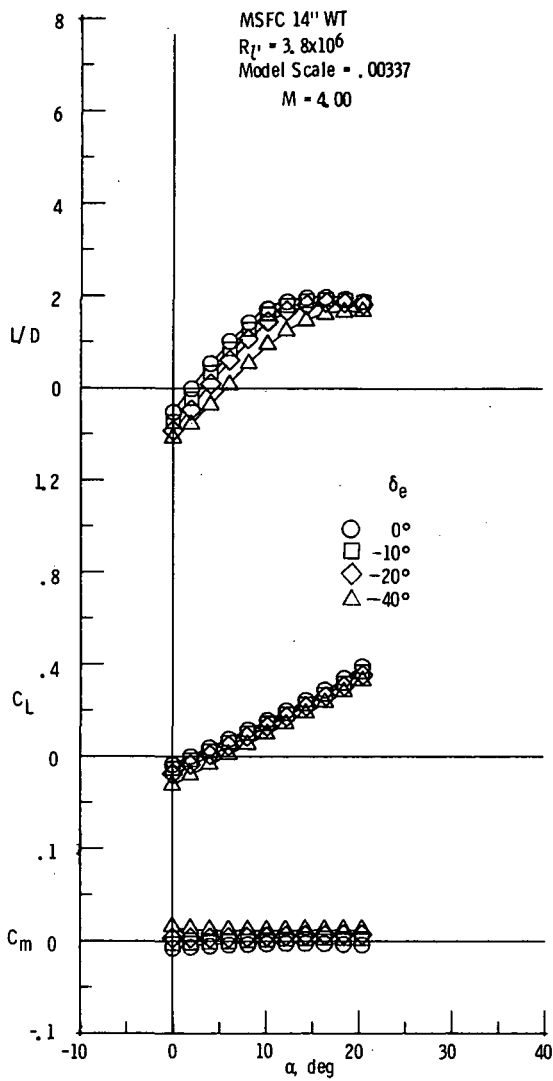
(c)  $1.60 \leq M \leq 2.16$ ;  $\delta_{rf} = 30^\circ$ .

Figure 3.- Continued.



(d)  $2.99 \leq M \leq 3.48$ ;  $\delta_{rf} = 30^\circ$ .

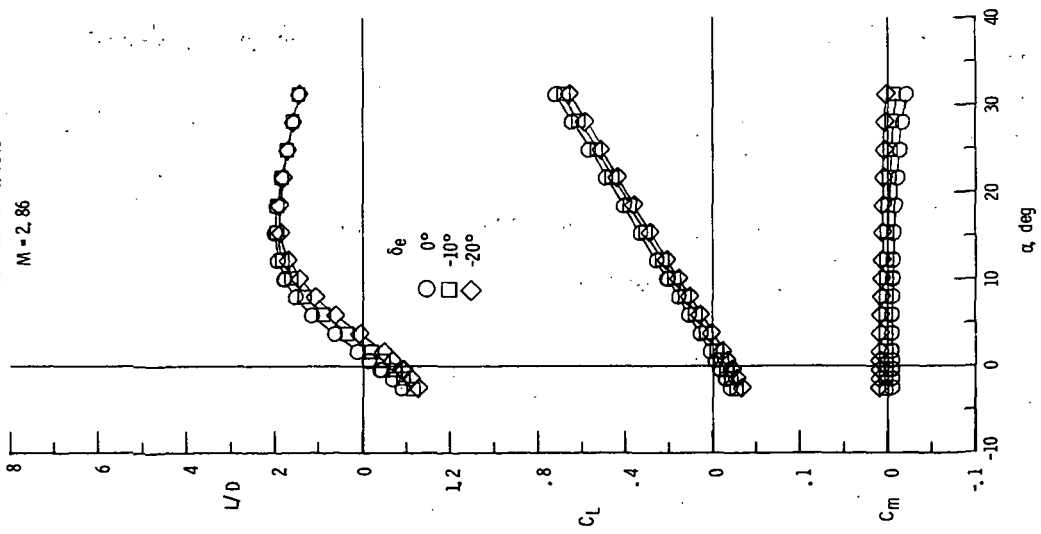
Figure 3. - Continued.



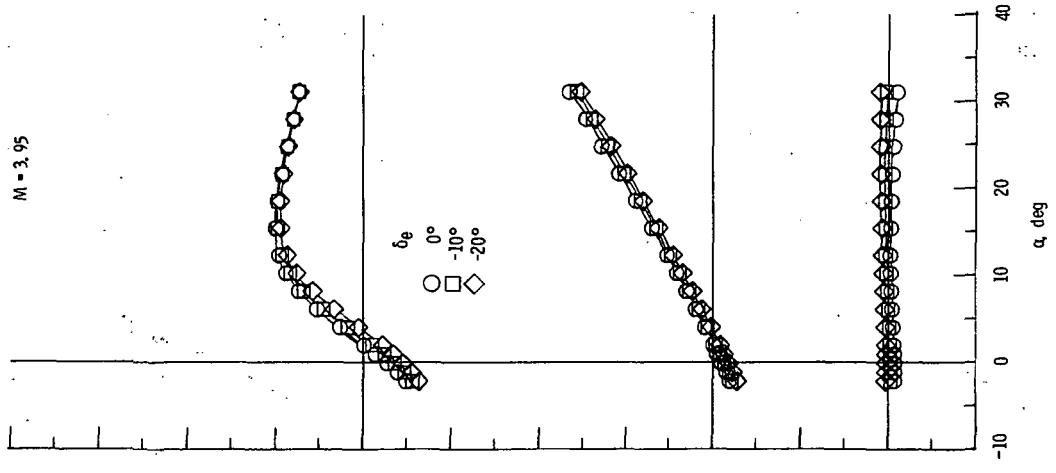
(e)  $4.00 \leq M \leq 4.96$ ;  $\delta_{rf} = 30^\circ$ .

Figure 3.- Continued.

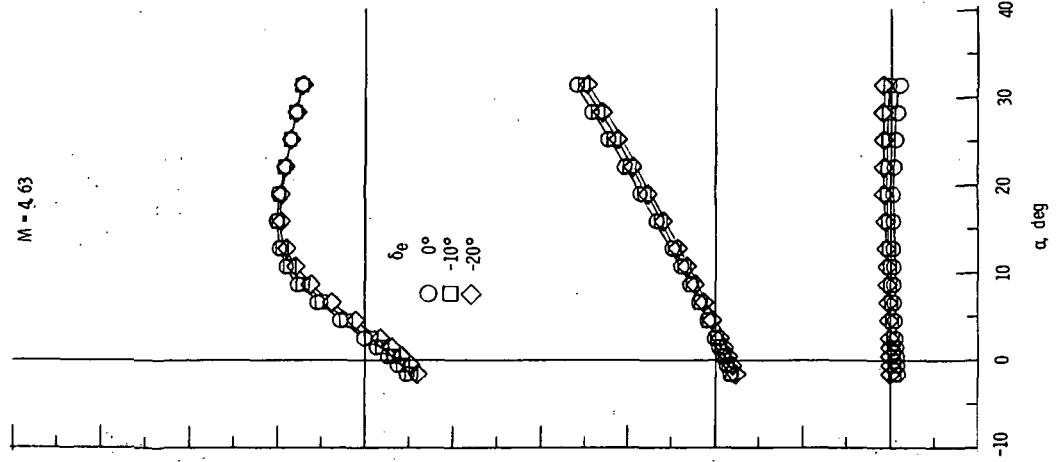
LaRC UPWT  
 $R_{T1} = 5.0 \times 10^6$   
 Model Scale = 0.0148  
 $M = 2.86$



LaRC UPWT  
 $R_{T1} = 5.0 \times 10^6$   
 Model Scale = 0.0148  
 $M = 3.95$

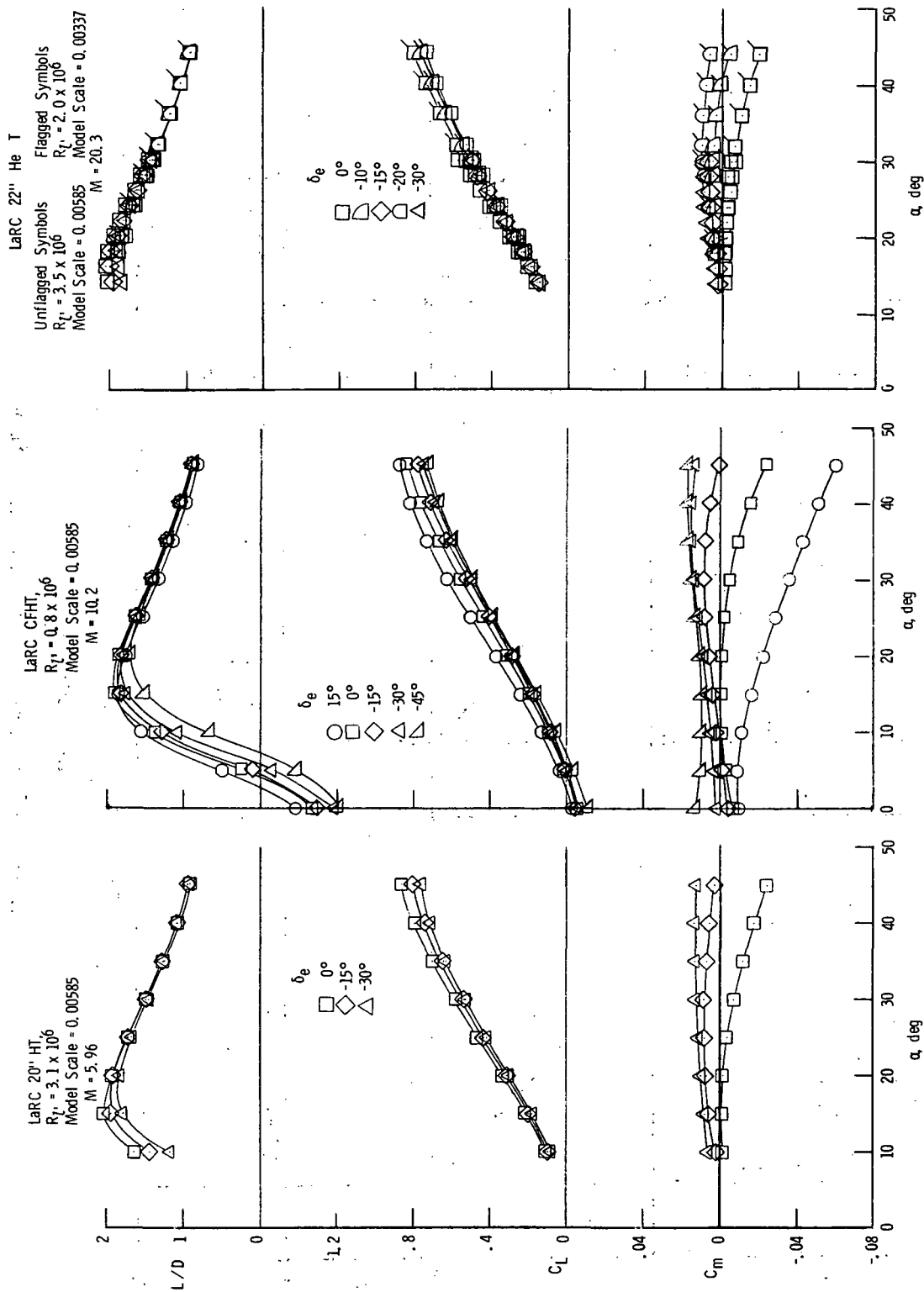


LaRC UPWT  
 $R_{T1} = 5.0 \times 10^6$   
 Model Scale = 0.0148  
 $M = 4.63$



(f)  $2.86 \leq M \leq 4.63$ ;  $\delta_{rf} = 30^\circ$ .

Figure 3.- Continued.



(g)  $5.96 \leq M \leq 20.3$ ;  $\delta_{rf} = 30^\circ$ .

Figure 3. - Concluded.

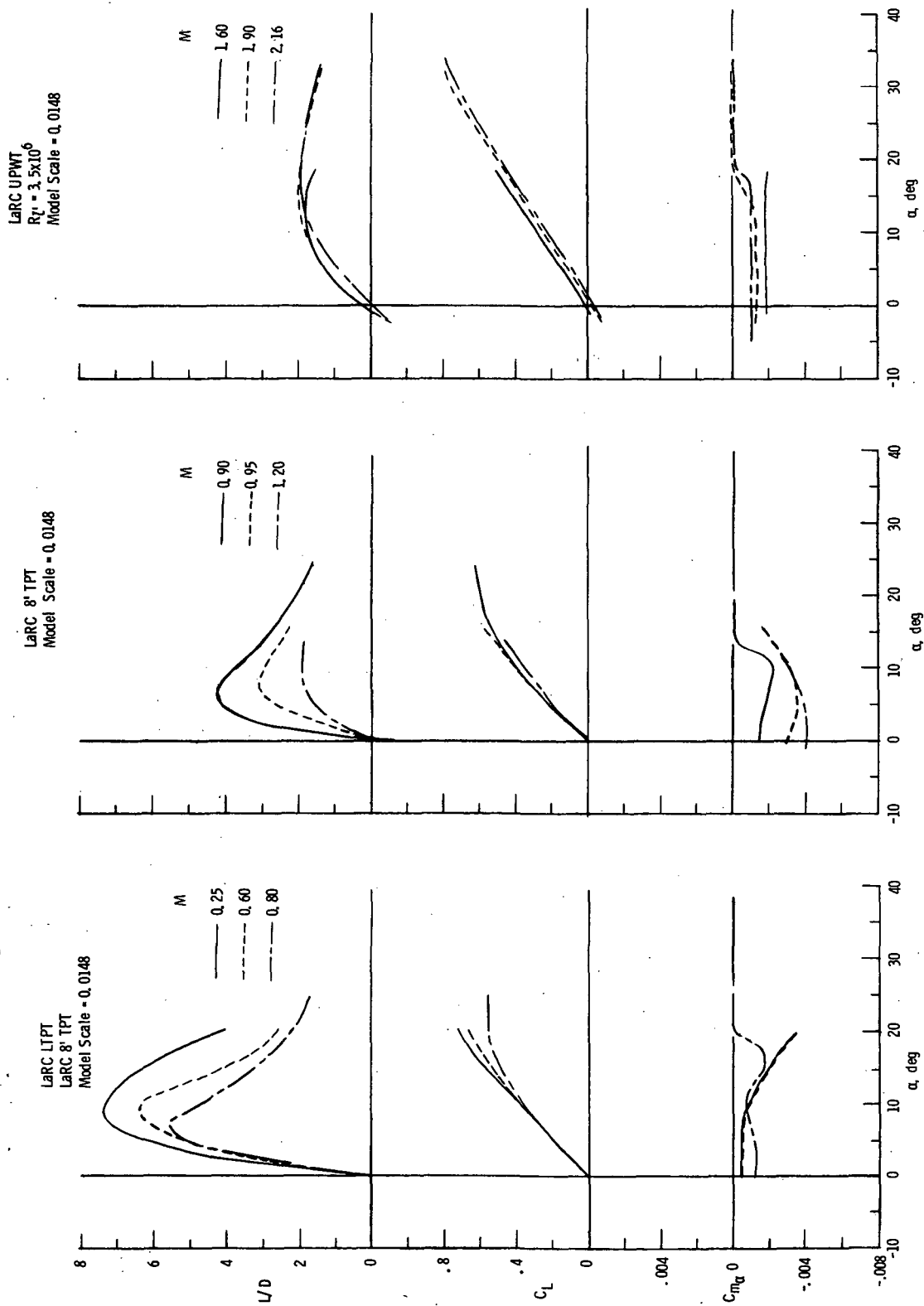
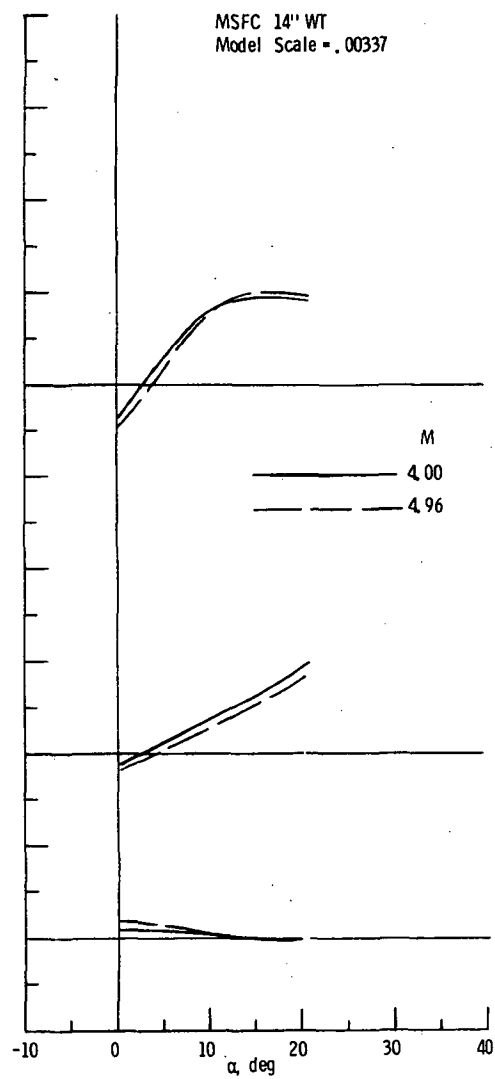
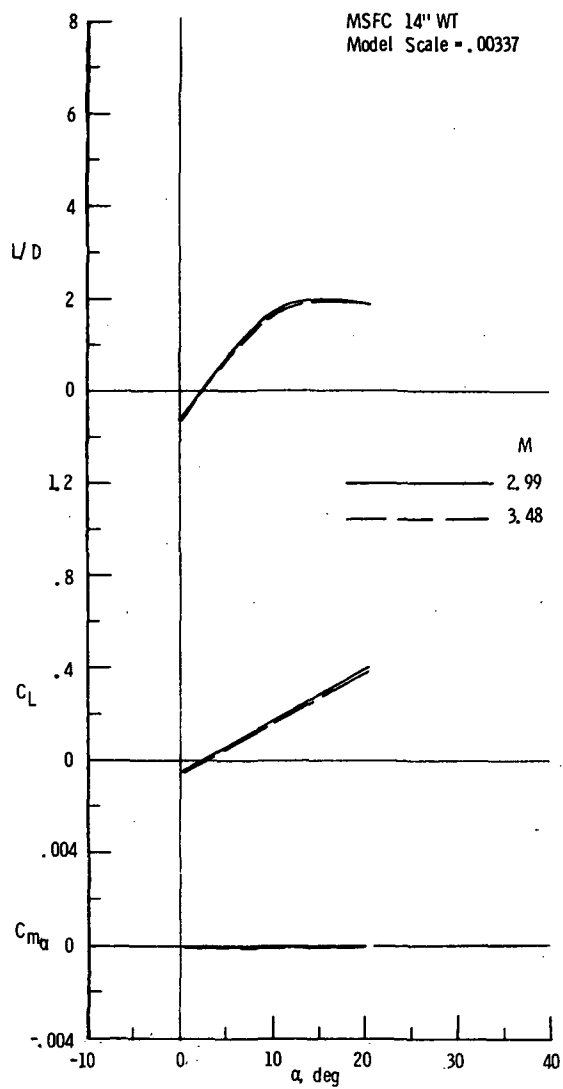
(a)  $0.25 \leq M \leq 2.16$ .

Figure 4. - Longitudinal trim characteristics.

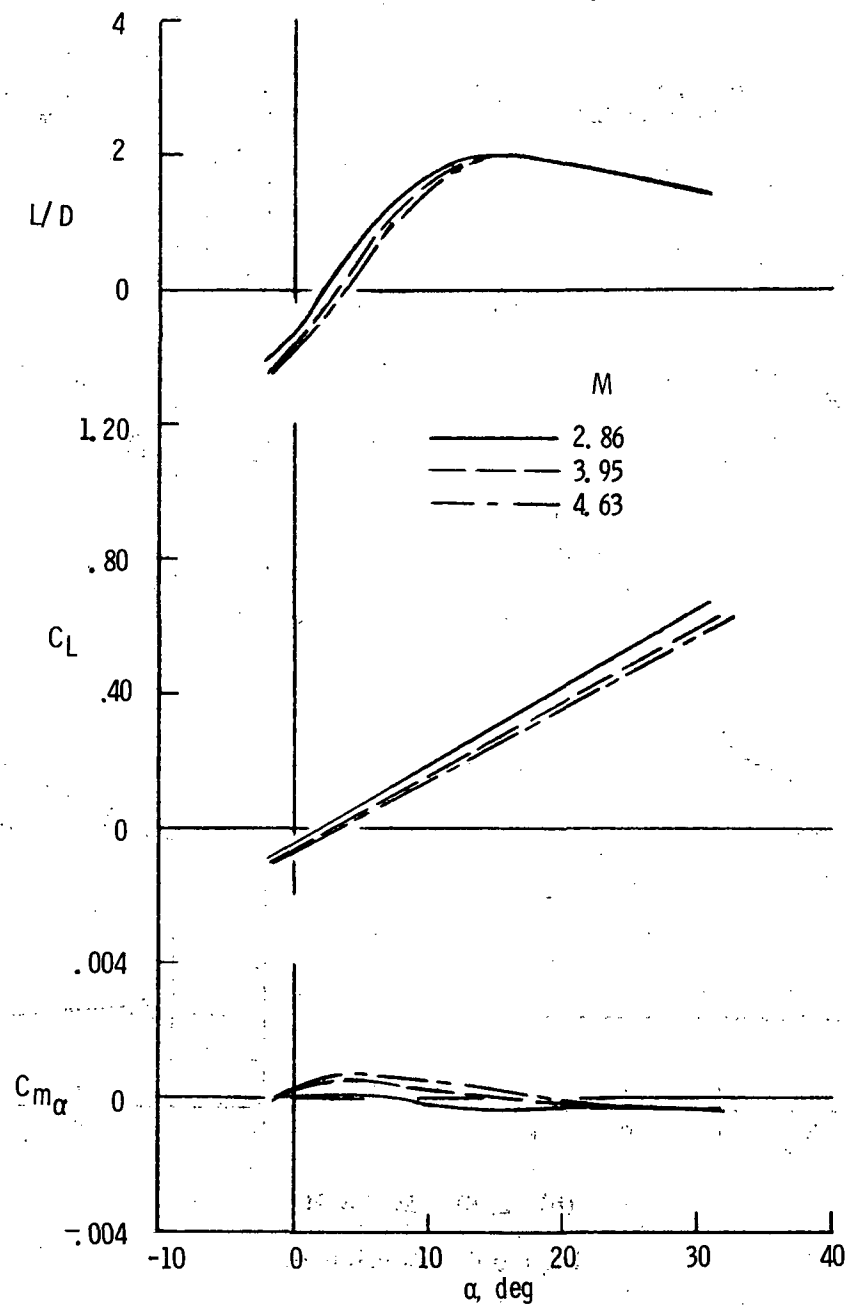




(b)  $2.99 \leq M \leq 4.96$ .

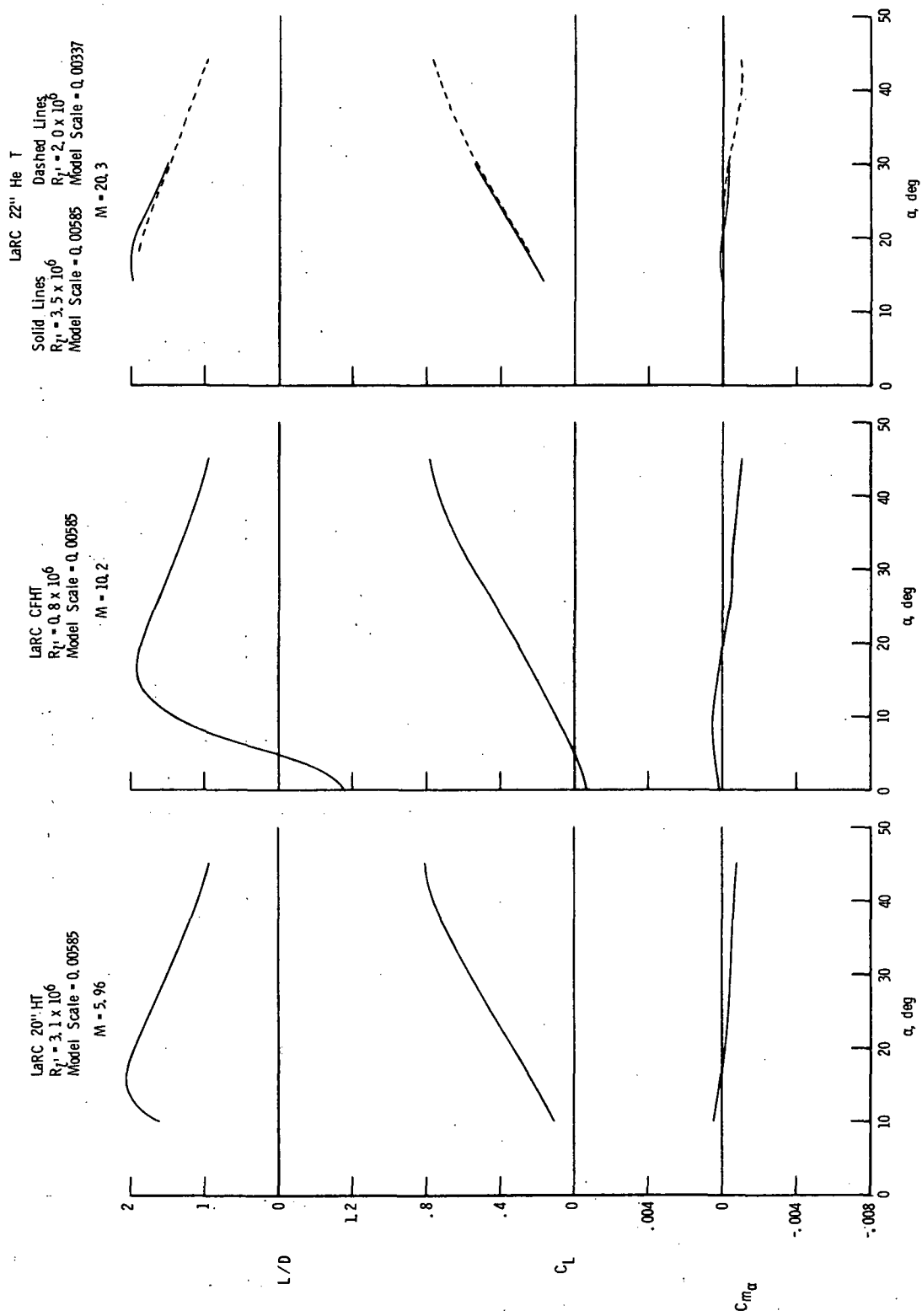
Figure 4.- Continued.

LaRC UPWT  
 $R_L = 5.0 \times 10^6$   
 Model Scale = 0.0148



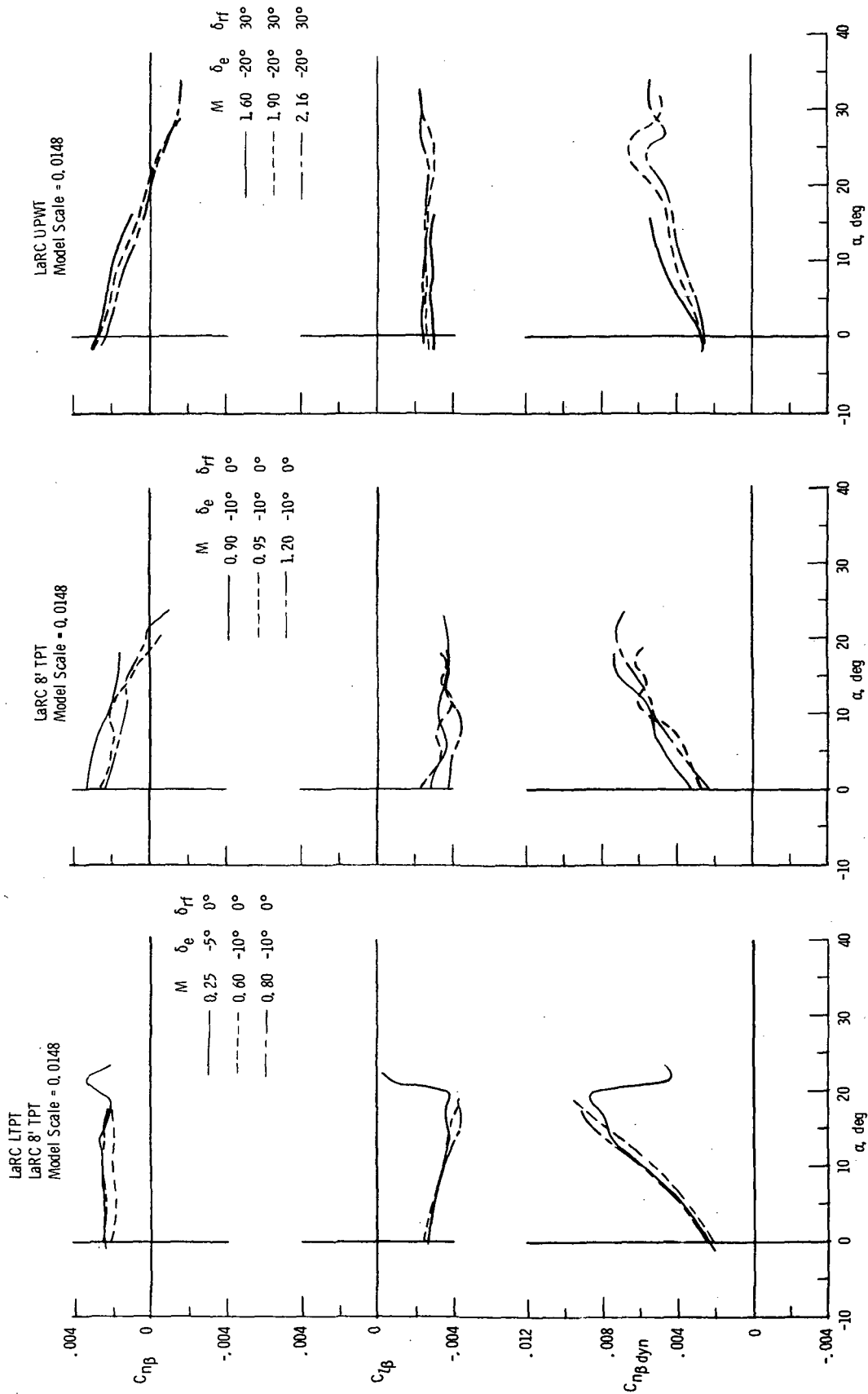
(c)  $2.86 \leq M \leq 4.63$ .

Figure 4.- Continued.



(d)  $5.96 \leq M \leq 20.3$ .

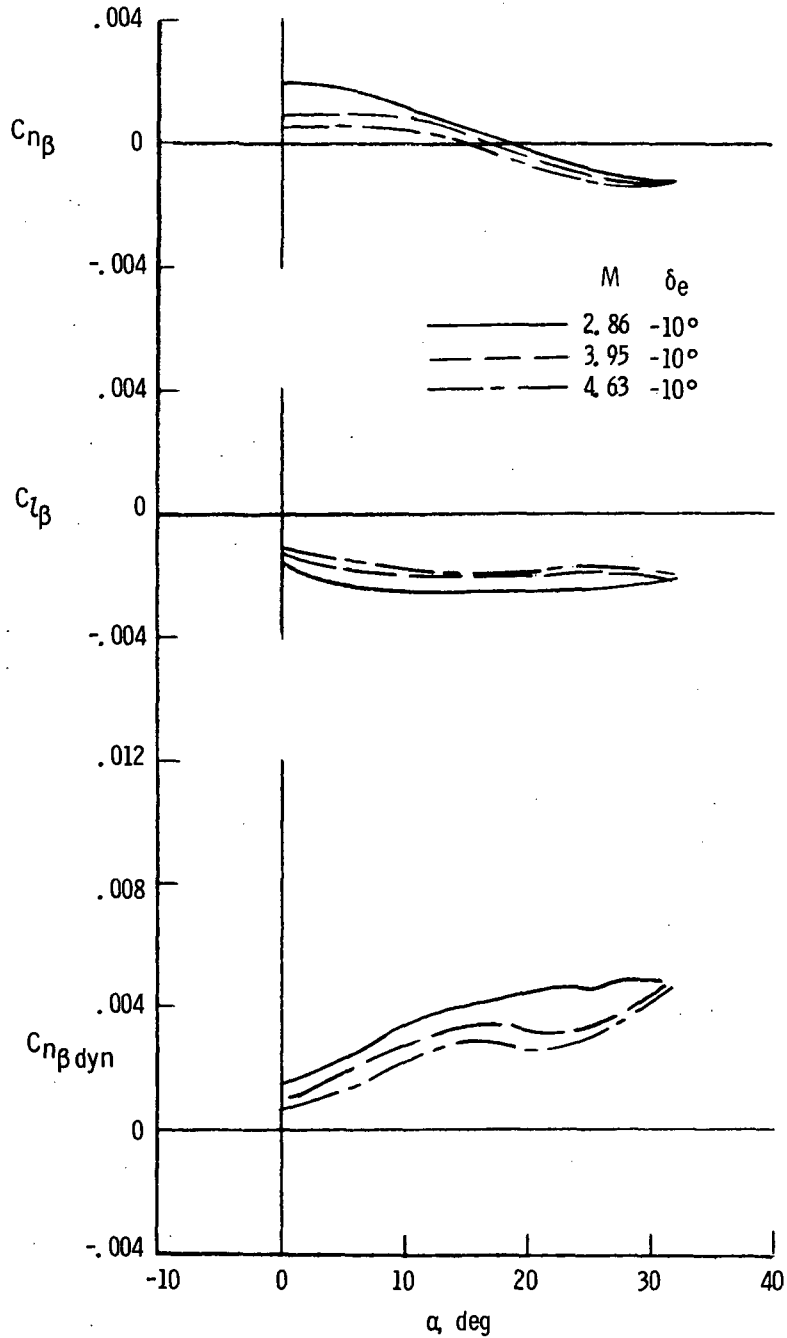
Figure 4.- Concluded.



(a)  $0.25 \leq M \leq 2.16$ .

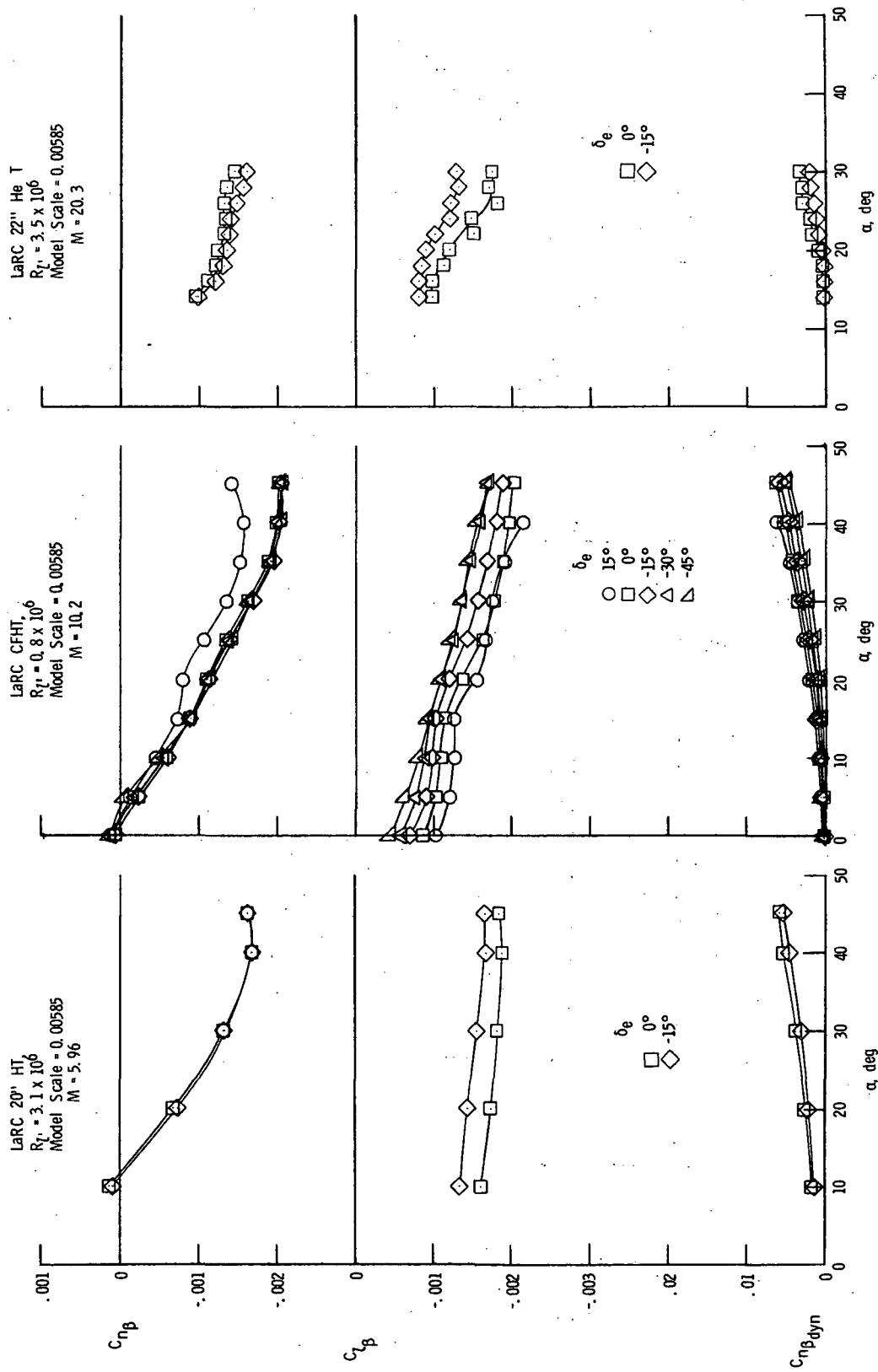
Figure 5.- Lateral-directional stability characteristics.  $\delta_r = 0^\circ$ .

LaRC UPWT  
 $R_{\ell'} = 5.0 \times 10^6$   
 Model Scale = 0.0148



(b)  $2.86 \leq M \leq 4.63$ ;  $\delta_{rf} = 30^\circ$ .

Figure 5.- Continued.



(c)  $5.96 \leq M \leq 20.3$ ;  $\delta_{rf} = 30^\circ$ .

Figure 5. - Concluded.

LaRC 20" HT,  
 $R_T = 3.1 \times 10^6$   
 Model Scale = 0.00585  
 $M = 5.96$

LaRC CFHT  
 $R_T = 0.8 \times 10^6$   
 Model Scale = 0.00585  
 $M = 10.2$

LaRC 22" He T  
 $R_T = 3.5 \times 10^6$   
 Model Scale = 0.00585  
 $M = 20.3$

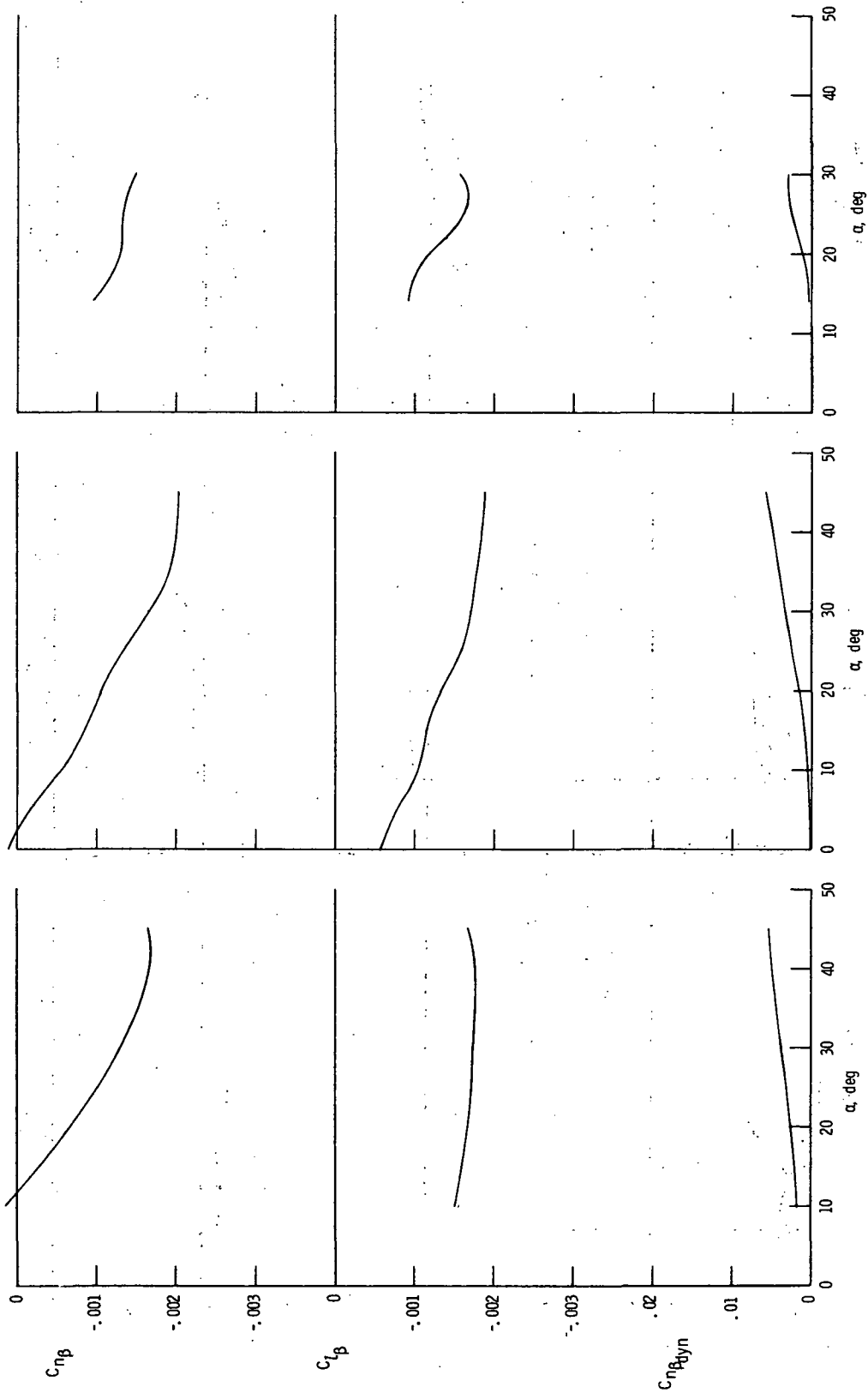
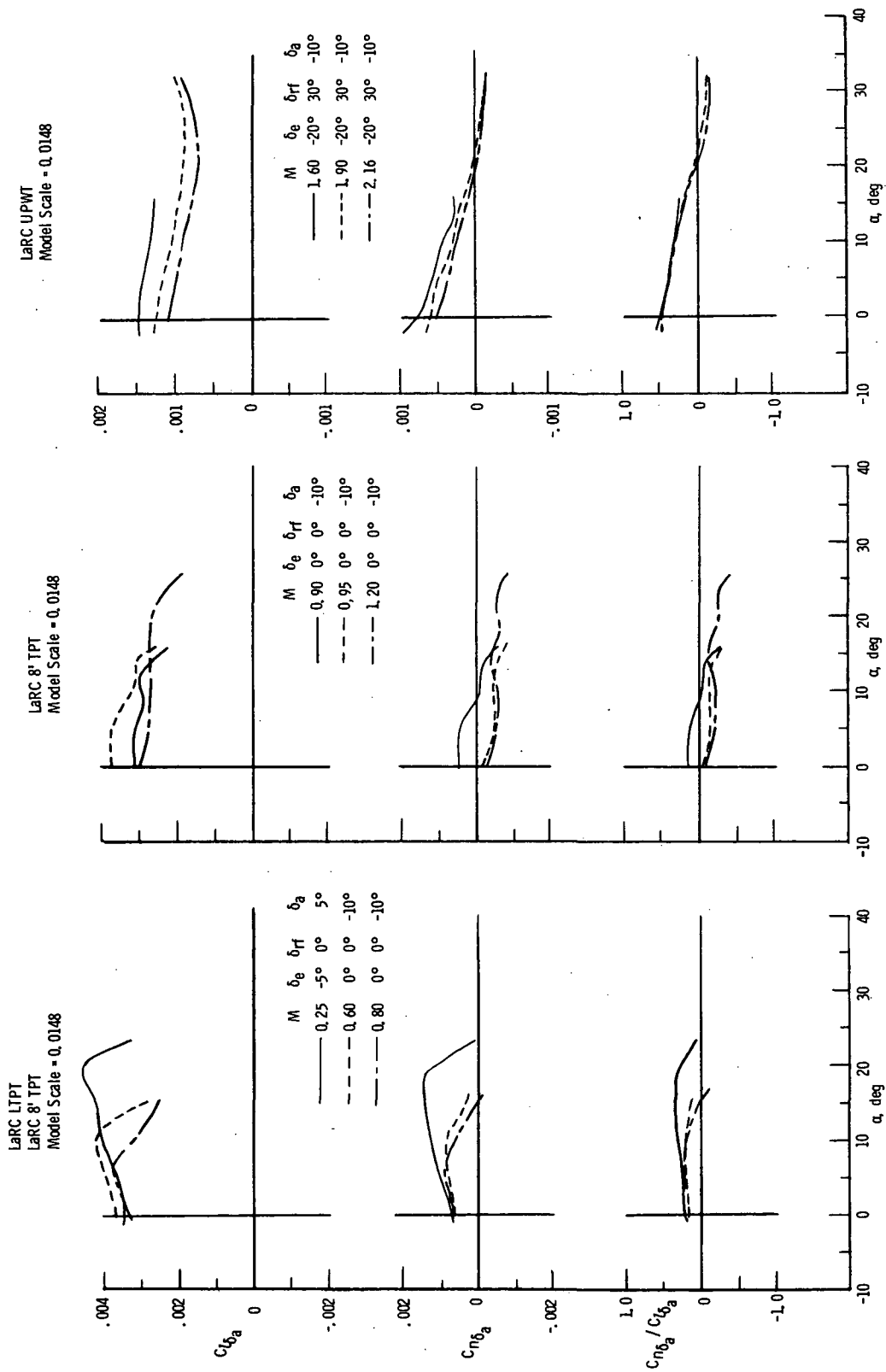


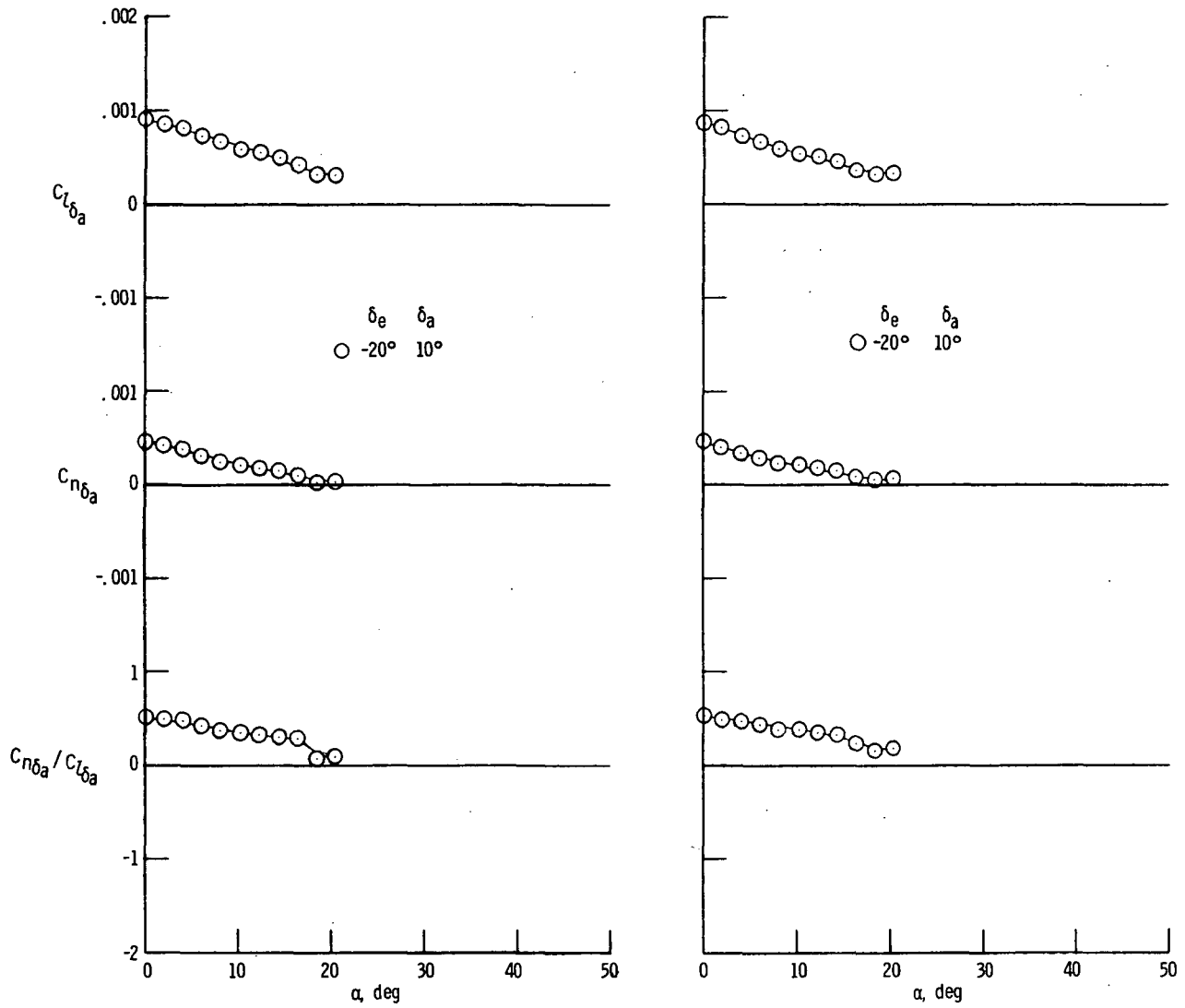
Figure 6. - Lateral-directional stability characteristics at longitudinal trim.

(a)  $0.25 \leq M \leq 2.16$ .Figure 7.- Roll-control characteristics.  $\delta_r = 0^\circ$ .



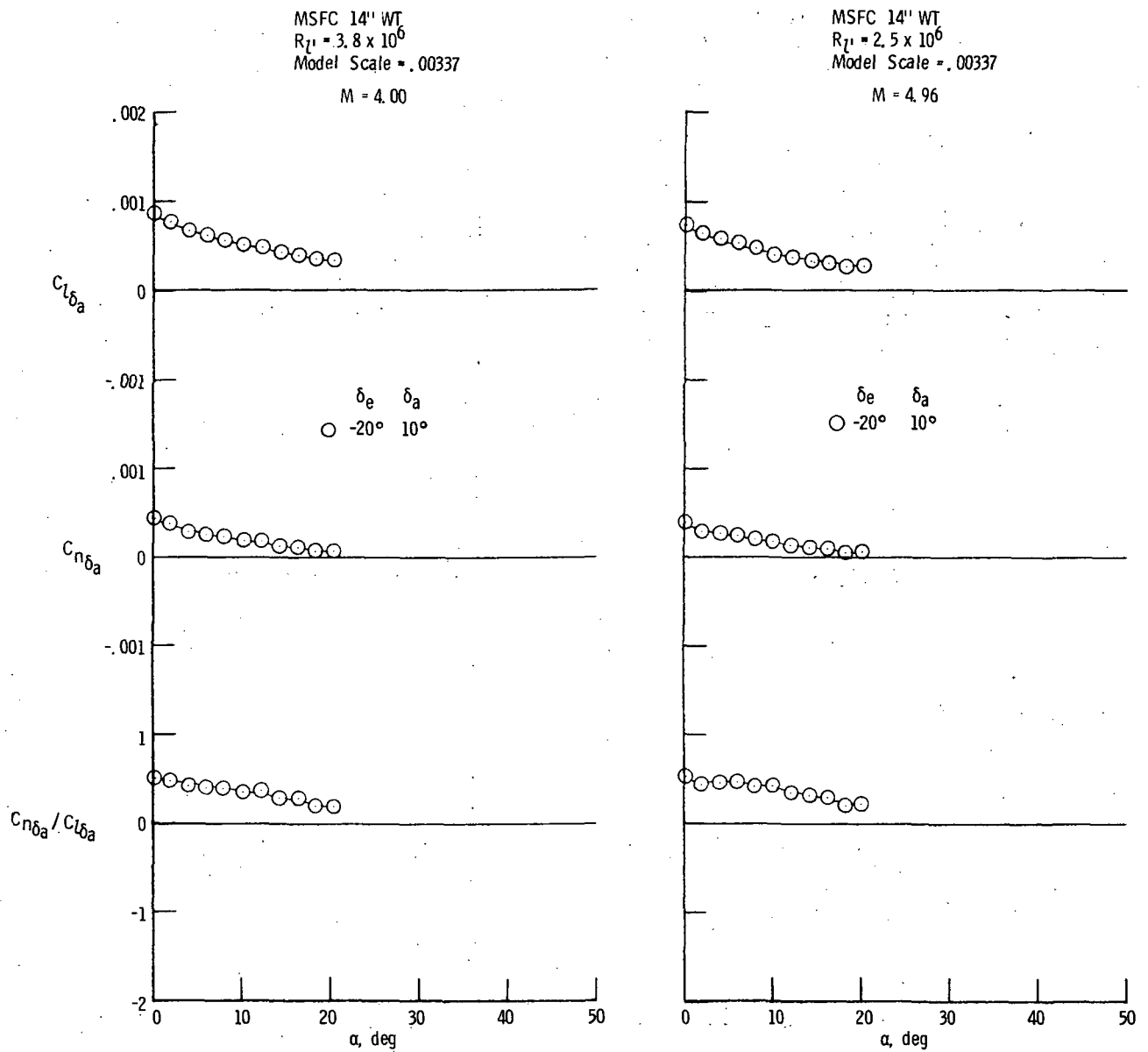
MSFC 14" WT  
 $R_{L'} = 2.4 \times 10^6$   
 Model Scale = .00337  
 $M = 2.99$

MSFC 14" WT  
 $R_{L'} = 3.2 \times 10^6$   
 Model Scale = .00337  
 $M = 3.48$



(b)  $2.99 \leq M \leq 3.48$ ;  $\delta_{rf} = 30^\circ$ .

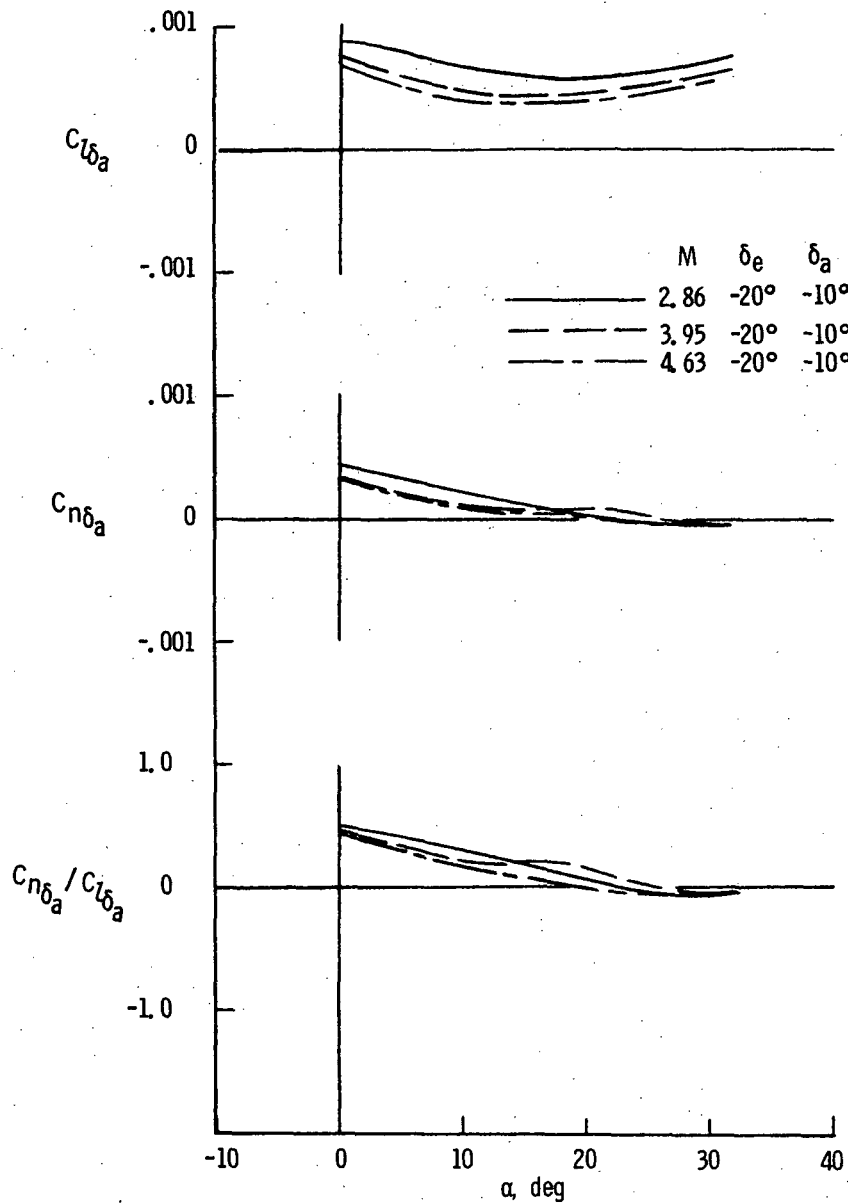
Figure 7.- Continued.



(c)  $4.00 \leq M \leq 4.96$ ;  $\delta_{rf} = 30^\circ$ .

Figure 7.- Continued.

LaRC UPWT  
 $R_L = 5.0 \times 10^6$   
 Model Scale = 0.0148



(d)  $2.86 \leq M \leq 4.63$ ;  $\delta_{rf} = 30^\circ$ .

Figure 7.- Continued.

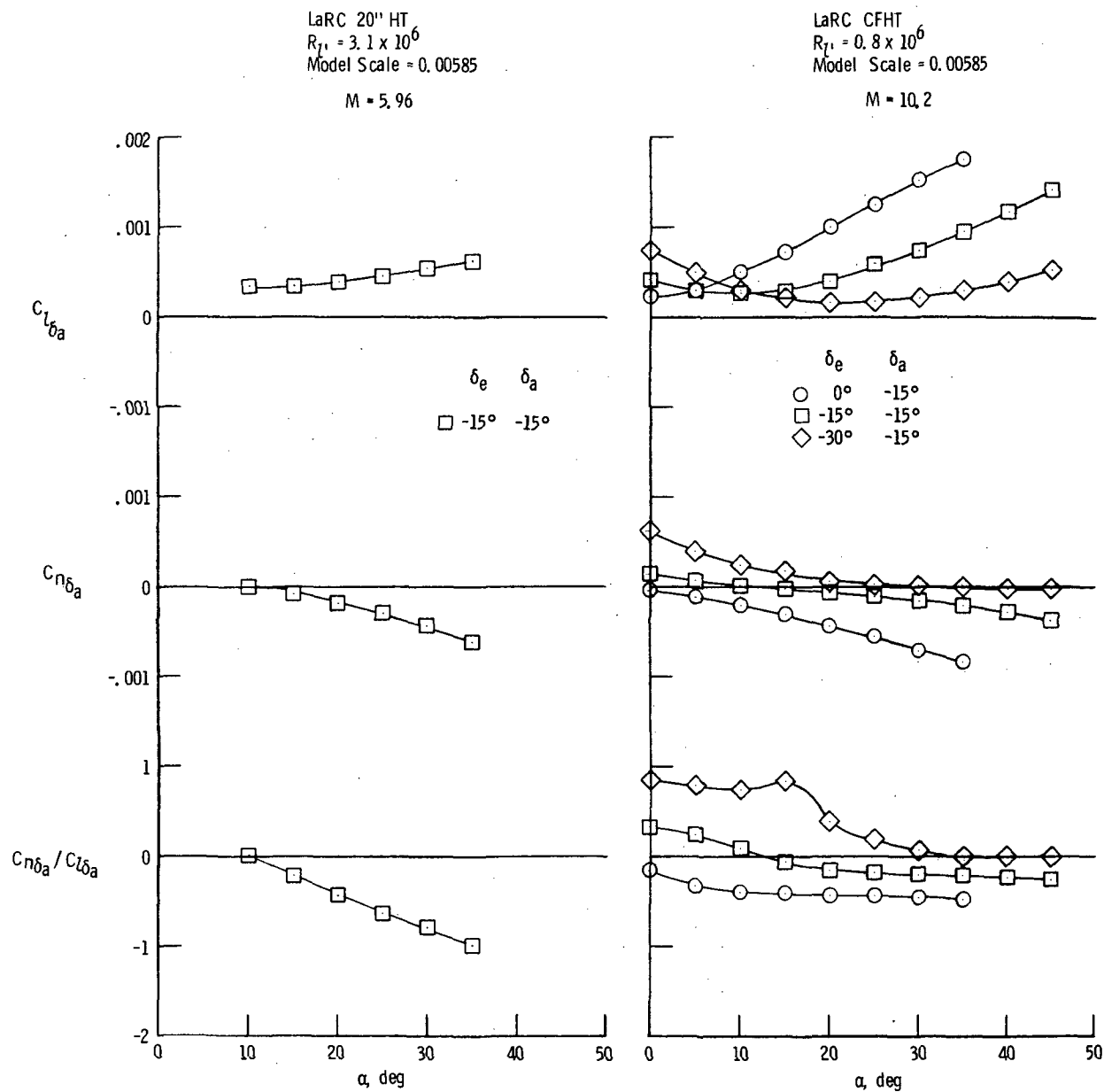
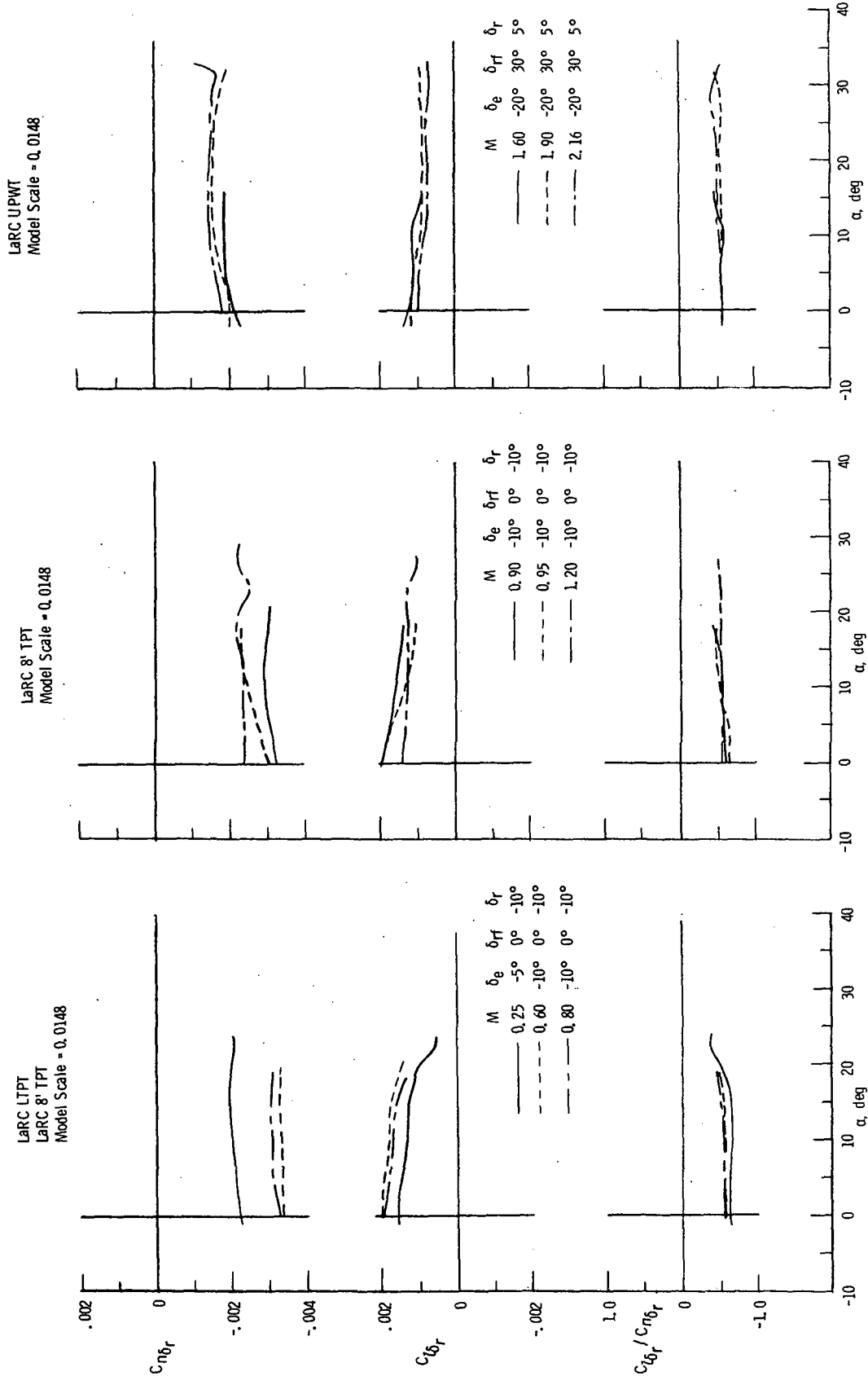


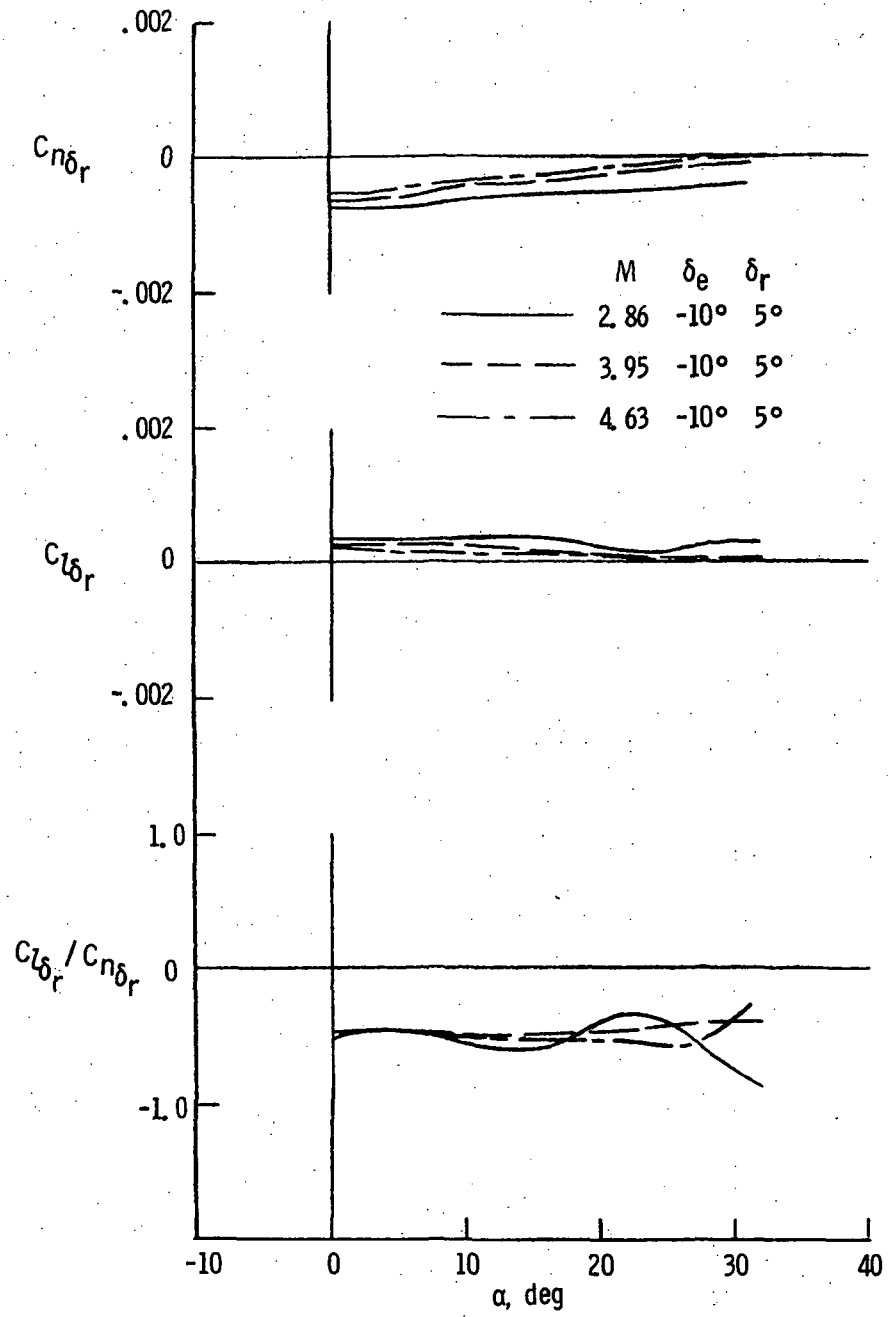
Figure 7.- Concluded.



(a)  $0.25 \leq M \leq 2.16$ .

Figure 8. - Directional control.

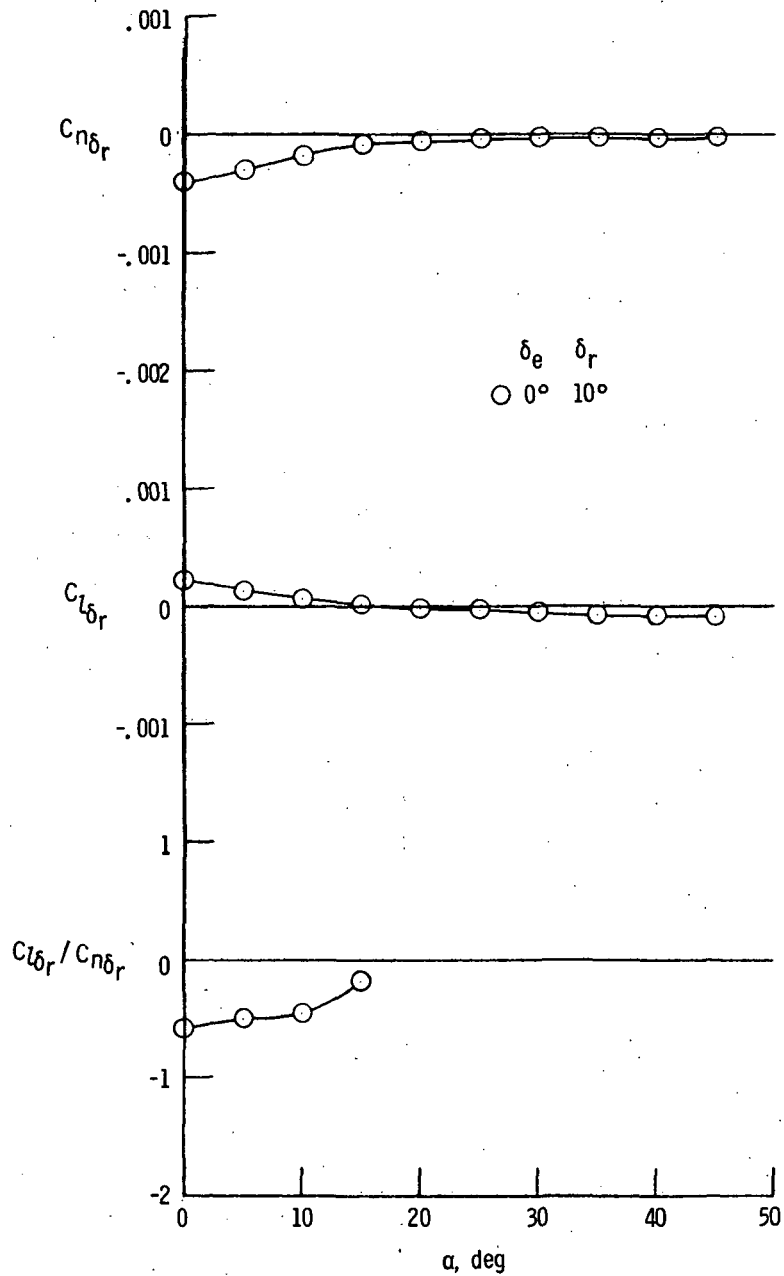
LaRC UPWT  
 $R_{\gamma} = 5.0 \times 10^6$   
 Model Scale = 0.0148



(b)  $2.86 \leq M \leq 4.63$ ;  $\delta_{rf} = 30^\circ$ .

Figure 8.- Continued.

LaRC CFHT  
 $R_{\rho} = 0.8 \times 10^6$   
 Model Scale = 0.00585  
 $M = 10.2$



(c)  $M \leq 10.2$ .

Figure 8.- Concluded.

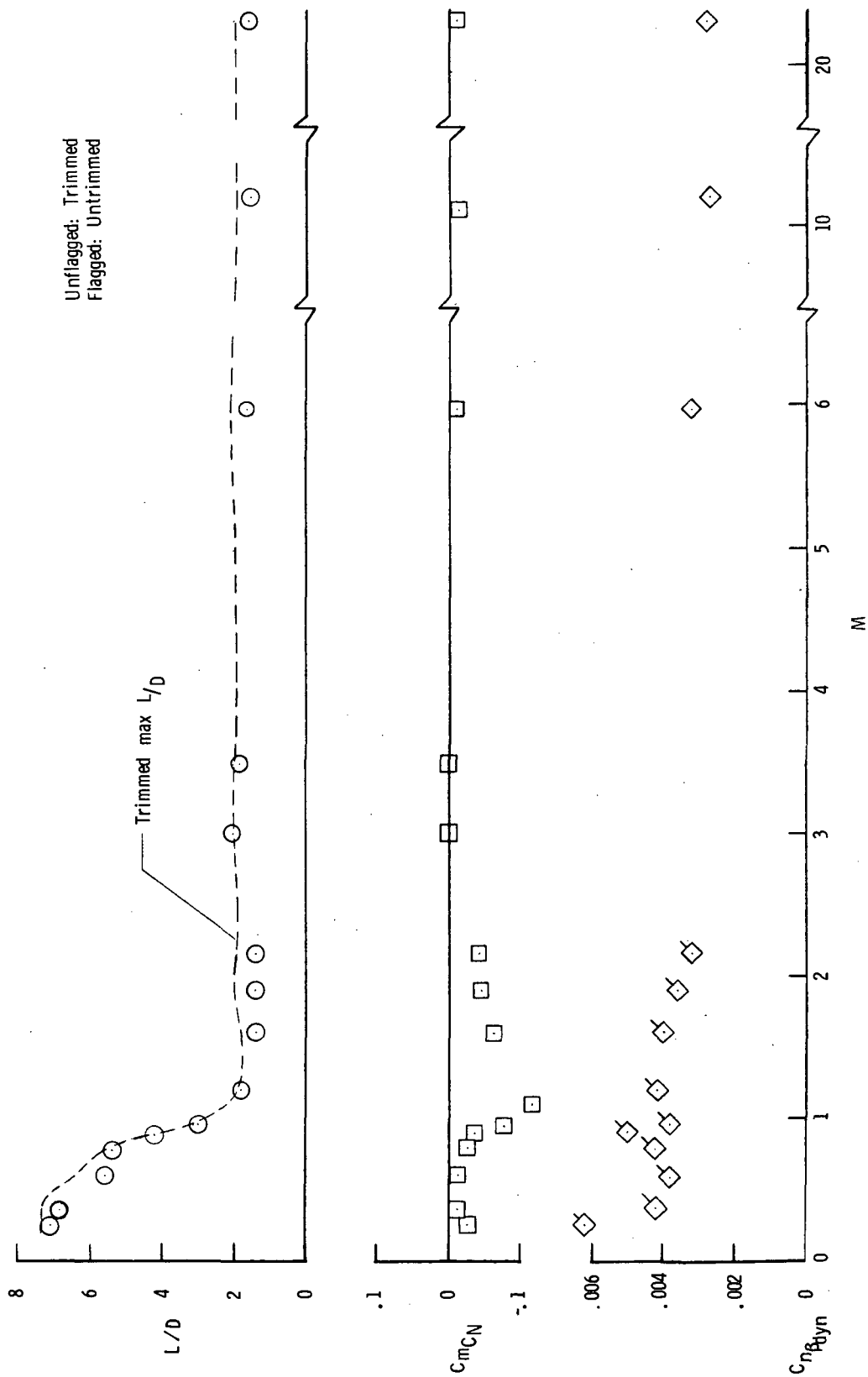
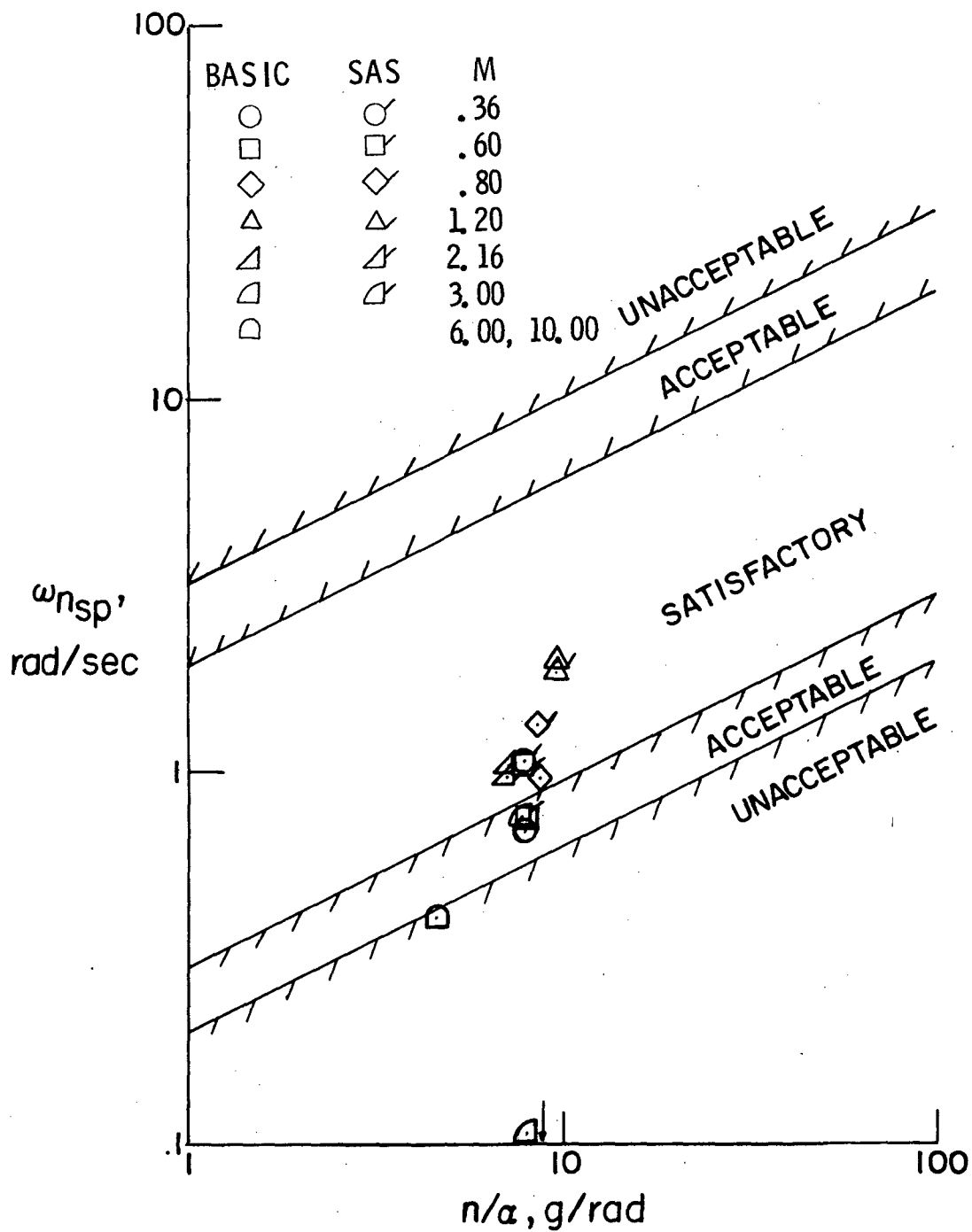


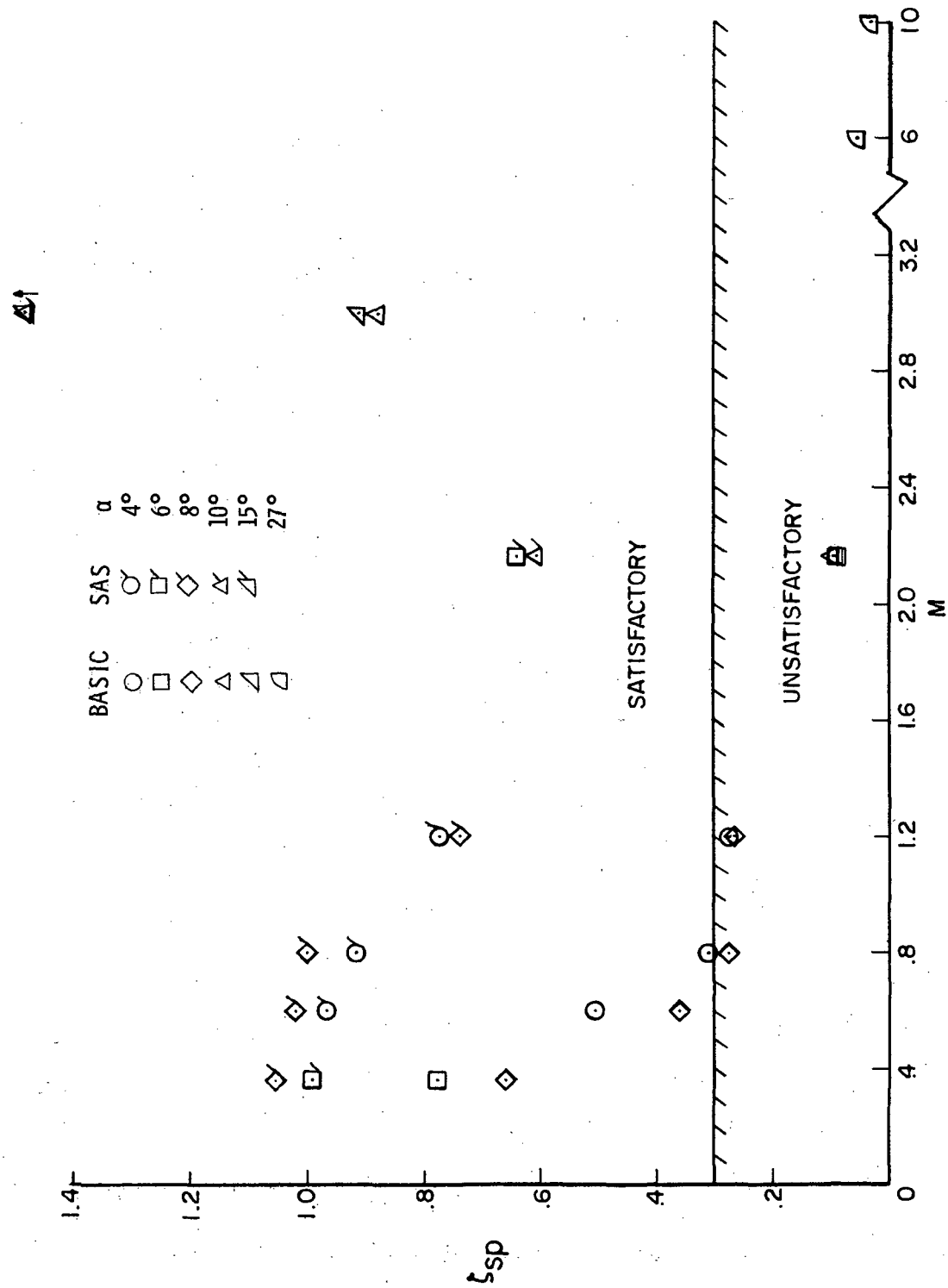
Figure 9. - Aerodynamic summary at operational flight attitudes.





(a) Short-period frequency.

Figure 10.- Longitudinal handling qualities (boundaries from ref. 6, class III, category B).



(b) Short-period damping ratio.

Figure 10. - Concluded.

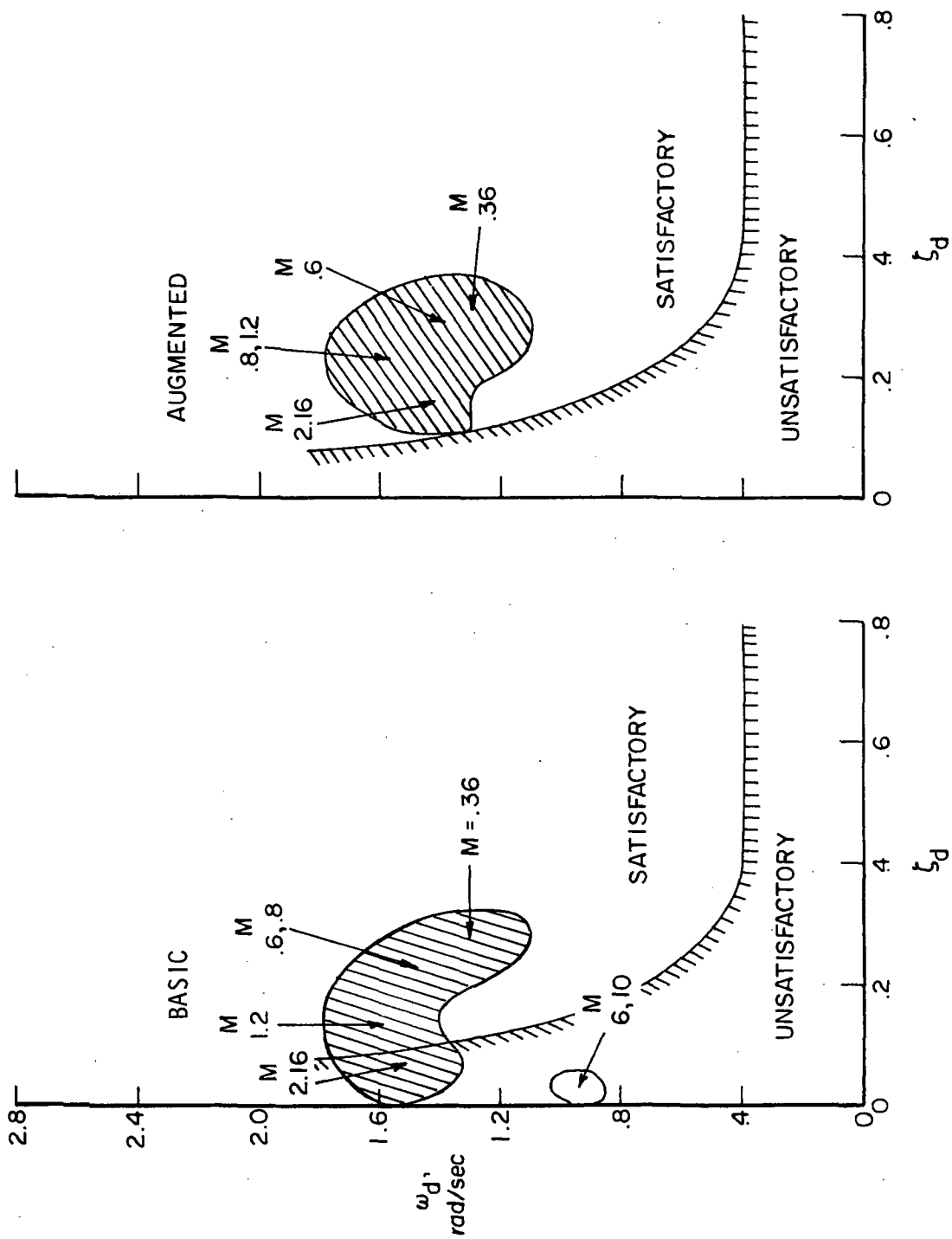


Figure 11. - Dutch roll mode characteristics.

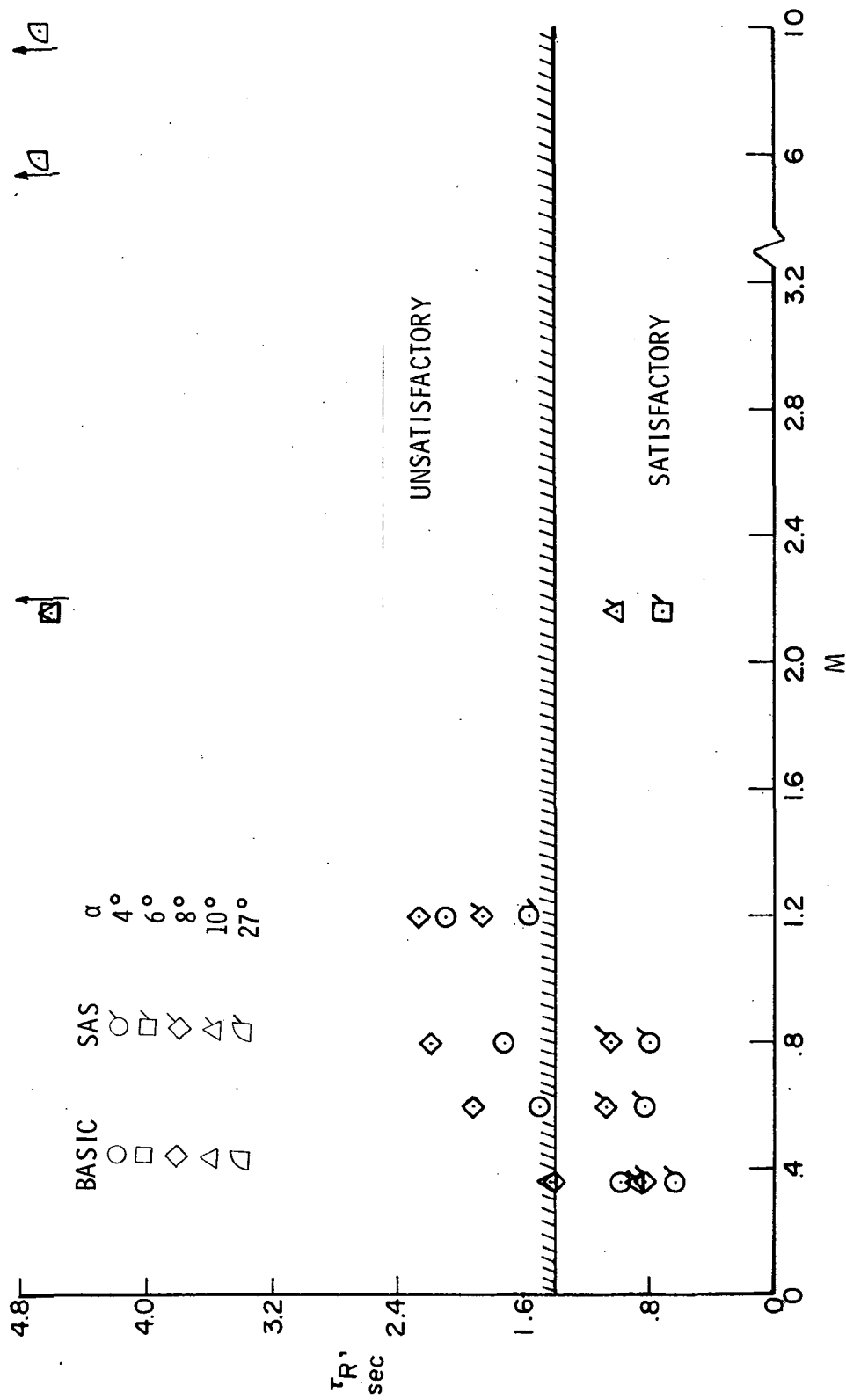


Figure 12. - Roll-mode time constant.

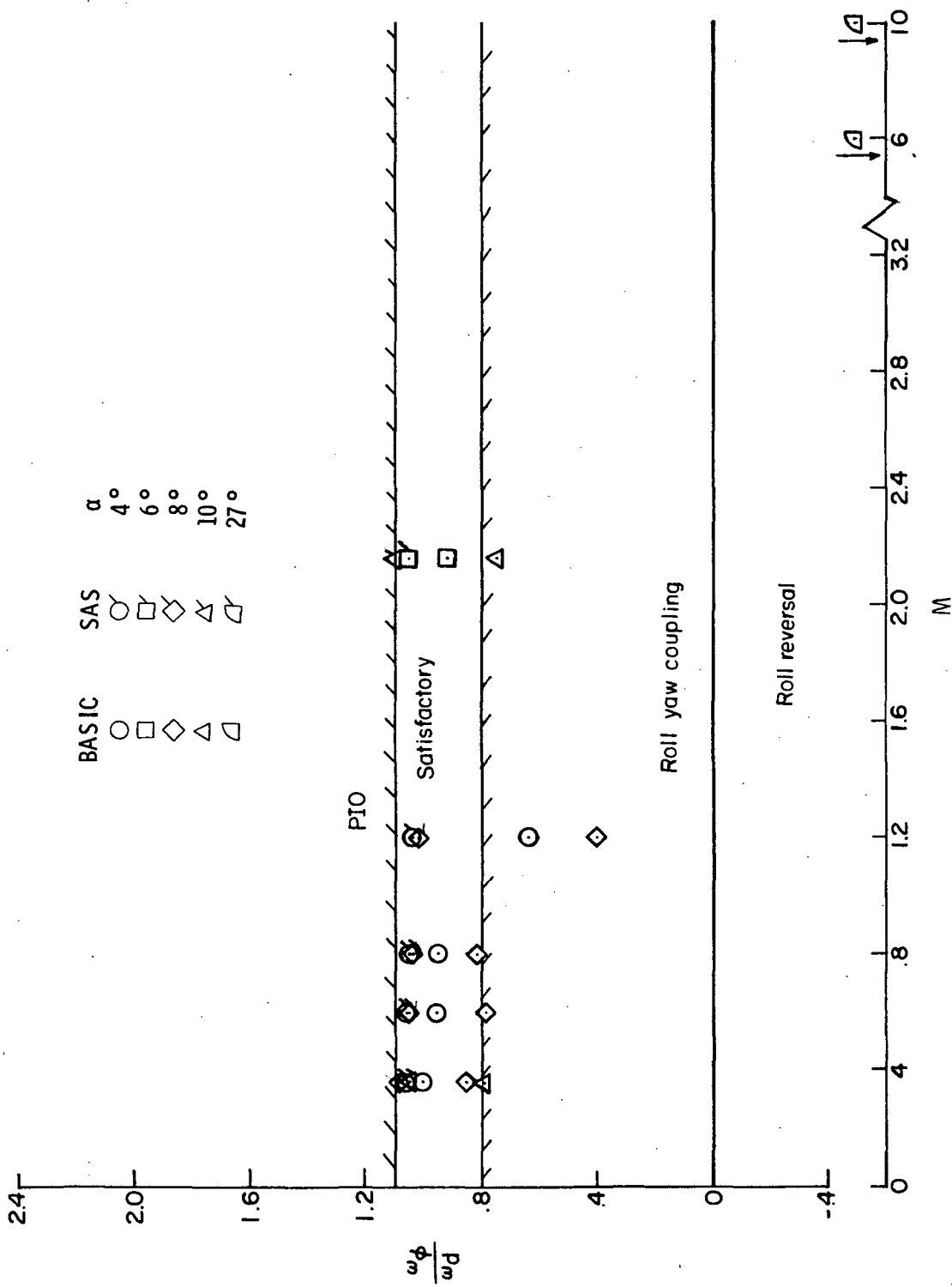


Figure 13.- Roll-coupling parameter.

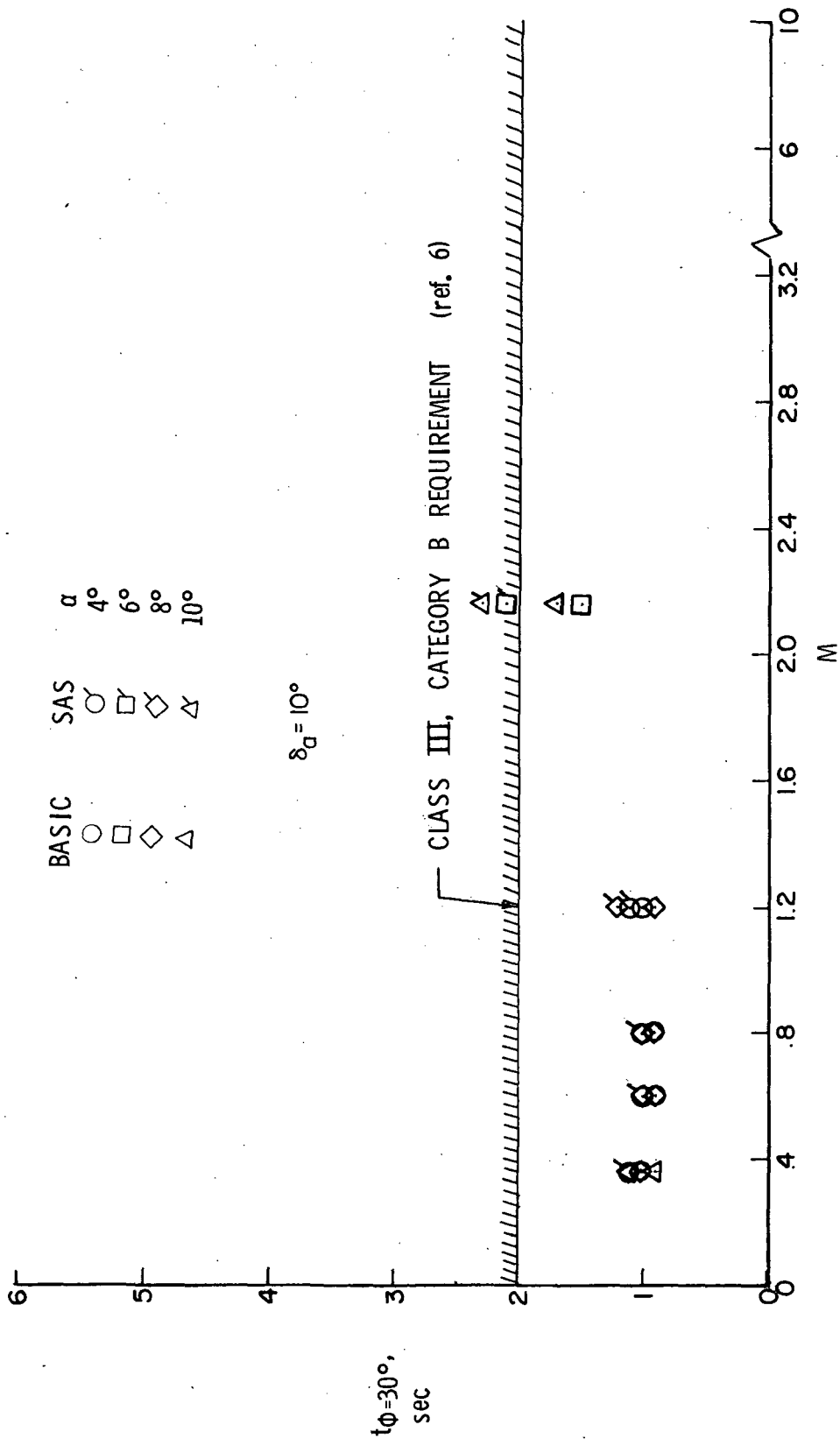
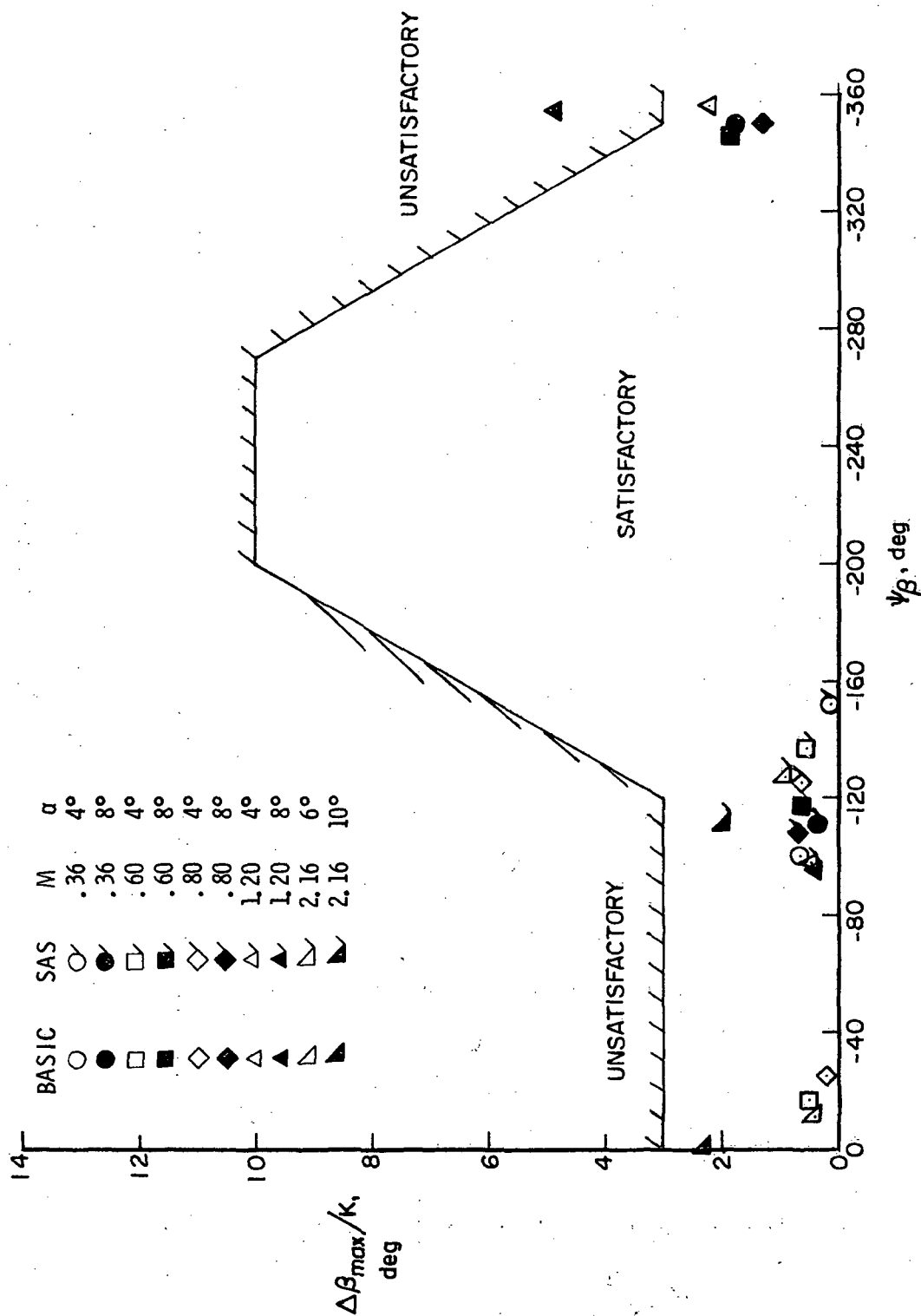
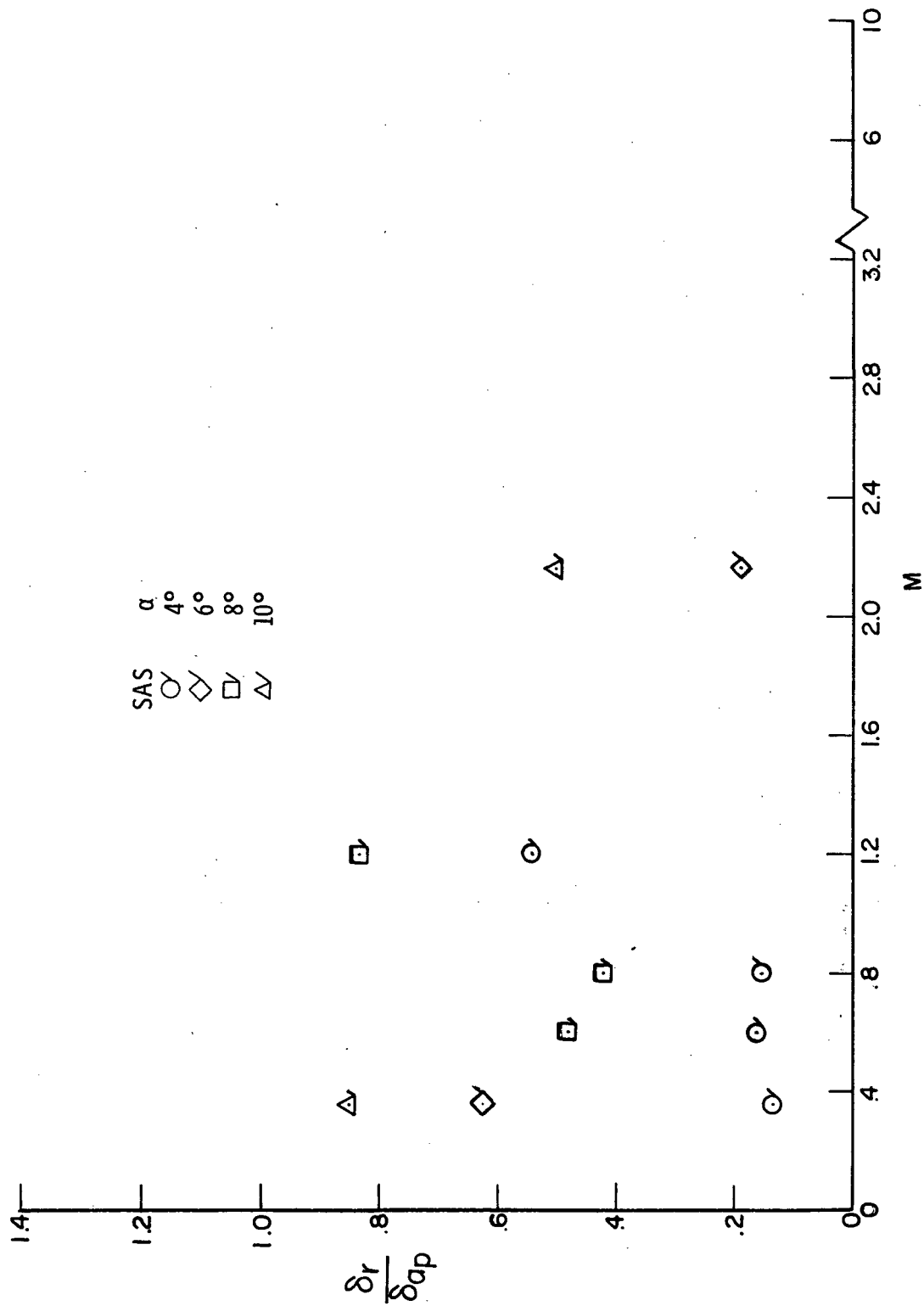
(a) Time to bank  $30^{\circ}$ .

Figure 14.- Rolling performance.



(b) Sideslip excursion limitations.

Figure 14.- Continued.



(c) Rudder requirements for coordinated turn.

Figure 14. - Concluded.





POSTMASTER: If Undeliverable (Section 158  
Postal Manual) Do Not Return

*"The aeronautical and space activities of the United States shall be conducted so as to contribute . . . to the expansion of human knowledge of phenomena in the atmosphere and space. The Administration shall provide for the widest practicable and appropriate dissemination of information concerning its activities and the results thereof."*

— NATIONAL AERONAUTICS AND SPACE ACT OF 1958

## NASA SCIENTIFIC AND TECHNICAL PUBLICATIONS

**TECHNICAL REPORTS:** Scientific and technical information considered important, complete, and a lasting contribution to existing knowledge.

**TECHNICAL NOTES:** Information less broad in scope but nevertheless of importance as a contribution to existing knowledge.

**TECHNICAL MEMORANDUMS:**  
Information receiving limited distribution because of preliminary data, security classification, or other reasons.

**CONTRACTOR REPORTS:** Scientific and technical information generated under a NASA contract or grant and considered an important contribution to existing knowledge.

**TECHNICAL TRANSLATIONS:** Information published in a foreign language considered to merit NASA distribution in English.

**SPECIAL PUBLICATIONS:** Information derived from or of value to NASA activities. Publications include conference proceedings, monographs, data compilations, handbooks, sourcebooks, and special bibliographies.

**TECHNOLOGY UTILIZATION PUBLICATIONS:** Information on technology used by NASA that may be of particular interest in commercial and other non-aerospace applications. Publications include Tech Briefs, Technology Utilization Reports and Technology Surveys.

*Details on the availability of these publications may be obtained from:*

**SCIENTIFIC AND TECHNICAL INFORMATION OFFICE**

**NATIONAL AERONAUTICS AND SPACE ADMINISTRATION**

**Washington, D.C. 20546**